UC Berkeley
UC Berkeley Previously Published Works

Title
Design and characterization of PROTAC degraders specific to protein N-terminal methyltransferase 1

Permalink
https://escholarship.org/uc/item/0143677f

Authors
Zhou, Qilong
Wu, Wei
Jia, Kaimin
et al.

Publication Date
2022-12-01

DOI
10.1016/j.ejmech.2022.114830

Copyright Information
This work is made available under the terms of a Creative Commons Attribution-NonCommercial-NoDerivatives License, available at https://creativecommons.org/licenses/by-nc-nd/4.0/

Peer reviewed

eScholarship.org Powered by the California Digital Library
University of California

Author Manuscript

Author Manuscript

Author Manuscript

Author Manuscript

HHS Public Access

Author manuscript

Eur J Med Chem. Author manuscript; available in PMC 2023 September 26.

Published in final edited form as:

Eur J Med Chem. 2022 December 15; 244: 114830. doi:10.1016/j.ejmech.2022.114830.

Design and Characterization of PROTAC Degraders Specific to Protein N-terminal Methyltransferase 1

Qilong Zhou[1,‡], **Wei Wu**[1,‡], **Kaimin Jia**[1,§], **Guangyan Qi**[2], **Xiuzhi Susan Sun**[2,3], **Ping Li**[1,*]

[1]Department of Chemistry, Kansas State University, Manhattan, Kansas, 66506, U.S.A.

[2]Department of Grain Science and Industry, Kansas State University, Manhattan, Kansas, 66506, U.S.A.

[3]Department of Biological and Agricultural Engineering, Kansas State University, Manhattan, Kansas, 66506, U.S.A.

Abstract

Protein N-terminal methylation catalyzed by N-terminal methyltransferase 1 (NTMT1) is an emerging methylation present in eukaryotes, playing important regulatory roles in various biological and cellular processes. Although dysregulation of NTMT1 has been linked to many diseases such as colorectal cancer, their molecular and cellular mechanisms remain elusive due to inaccessibility to cellular probes. Here we report the design, synthesis, and characterization of the first-in-class NTMT1 degraders based on proteolysis-targeting chimera (PROTAC) strategy. Through a brief structure-activity relationship (SAR) study of linker length, a cell permeable degrader **1** involving a von Hippel-Lindau (VHL) E3 ligase ligand was developed and demonstrated to reduce NTMT1 protein levels effectively and selectively in time- and dose-dependent manners in colorectal carcinoma cell lines HCT116 and HT29. Degrader **1** displayed DC_{50} = 7.53 μM and D_{max} > 90% in HCT116 (cellular IC_{50} > 100 μM for its parent inhibitor DC541). While degrader **1** had marginal cytotoxicity, it displayed anti-proliferative activity in 2D and 3D culture environment, resulting from cell cycle arrested at G0/G1 phase in HCT116. Label-free global proteomic analysis revealed that degrader **1** induced overexpression of calreticulin (CALR), an immunogenic cell death (ICD) signal protein that is known to elicit antitumor immune response and clinically linked to a high survival rate of patients with colorectal cancer upon its upregulation. Collectively, degrader **1** offers the first selective cellular probe for NTMT1 exploration and a new drug discovery modality for NTMT1-related oncology and diseases.

Keywords

antiproliferative effect; calreticulin (CALR); cellular probe; colorectal carcinoma HCT116; N-terminal methyltransferases 1 (NTMT1); PROTAC

*Corresponding author: pli@k-state.edu.

‡These authors contributed equally.

§Current address: Department of Chemical and Biomolecular Engineering, University of California, Berkeley, CA, 94720, U.S.A

DECLARATION OF INTERESTS

The authors declare no competing financial interest.

SUPPLEMENTARY DATA

Supplementary data to this article can be found online

Author Manuscript Author Manuscript Author Manuscript Author Manuscript

INTRODUCTION

Protein N-terminal methylation is an emerging methylation that involves addition of 1 to 3 methyl groups from *S*-adenosyl-*L*-methionine (SAM) onto the exposed α-amino group of the protein N-terminus with a concurrent release of *S*-adenosine-*L*-homocysteine (SAH).[1–4] While this modification was first discovered four decades ago,[5–7] it is largely unexplored until recent discovery of NTMT1 in yeast and human.[8–9] Studies including ours have indicated that NTMT1-catalyzed protein N-terminal methylation is widespread in histone and non-histone proteins,[8–20] which has been shown to play critical roles in regulation of cell mitosis, chromatin interactions, DNA repair, tRNA transport, and genome stability.[14–15, 17–18, 20–21] Given the importance of N-terminal methylation in various biological processes, it is not surprising that its dysregulation has been linked to many diseases such as malignant melanoma and colorectal, breast, lung, and brain cancers.[22–25] Particularly, NTMT1 was found to be robustly overexpressed in patients with colorectal cancer and ranked in the top 1% of all proteins undergoing expression level changes.[26–28] Moreover, knockout of *ntmt1* gene in human colorectal carcinoma HCT116 caused pronounced defects in cell proliferation.[23] All of these suggest that NTMT1 may act as an oncogene and potential drug target of colorectal cancer,[23] which is the third most diagnosed cancer and the fourth leading cause of death worldwide.[29]

Much of recent effort has been focused on developing inhibitors to NTMT1,[30–35] which are pivotal not only for advancing their applications into therapeutics, but also for understanding molecular and cellular mechanisms of protein N-terminal methylation. While several NTMT1 inhibitors have shown potent inhibition at nM to sub-nM ranges *in vitro*, none of them displayed satisfactory cellular activity.[33–35] PROTACs have recently emerged as an attractive technology to employ small molecules for targeted protein degradation.[36–37] Chemical conversion of previously characterized inhibitors into PROTAC degraders has been utilized in drug discovery and shown great therapeutic advantages such as improved potency, prolonged pharmacodynamics, and in some cases, improved selectivity.[38–45] Therefore, we decided to employ PROTAC as a strategy to develop NTMT1 degraders in hope for enhanced cellular and therapeutic activities toward colorectal carcinoma cells.

Here we report the design, synthesis, and characterization of the first-in-class NTMT1 degraders. Through a brief structure-activity relationship (SAR) study of linker length, a cell permeable degrader **1** was developed by connecting a reported NTMT1 peptidomimetic inhibitor, DC541,[33] to a VHL E3 ligase ligand. While DC541 had cellular IC_{50} > 100 μM in HCT116,[33] degrader **1** displayed DC_{50} = 7.53 μM and D_{max} > 90% in the same cell line. The NTMT1-selective degradation was visualized by fluorescence and shown to be time- and dose-dependent. Degrader **1** could also inhibit proliferation of cancer cells in 2D and 3D culture environment, for which the cells were found to be arrested at G0/G1 phase. Moreover, label-free global proteomic analysis using mass spectrometry (MS) revealed that treatment of HCT116 with degrader **1** induced overexpression of an immunogenic cell death (ICD) signal protein named calreticulin (CALR), which was also confirmed by Western blot. Taken together, the first-in-class NTMT1 degraders presented here provides not only a new class of effective and selective cellular probe to uncover biological and

Author Manuscript Author Manuscript Author Manuscript Author Manuscript

physiological functions of N-terminal methylation, but also a new therapeutic strategy for potential treatment of diseases involving NTMT1.

RESULTS AND DISCUSSION

PROTAC design and synthesis.

PROTAC has emerged as a novel and appealing strategy in drug discovery with several potential advantages relative to a traditional occupancy-driven approach. As depicted in Figure 1A, PROTAC employs a heterobifunctional molecule (called degrader) that recruits both the protein of interest (POI) and E3 ubiquitin ligase to form a ternary complex. Subsequent polyubiquitination of the POI by ubiquitination machinery initiates the recognition and ensuing degradation by 26S proteasome, which is a part of ubiquitin-proteasome system (UPS) in eukaryotic cells.[36–37] Unlike an occupancy-driven approach that requires at least stoichiometric amount of an enzyme inhibitor, degradation induced by PROTAC is a catalytic cycle.[46] Therefore, degraders can operate at much lower doses for their targets than traditional occupancy-driven inhibitors, eliciting less opportunity for the POIs to undergo mutation and develop drug resistance.[40, 43, 47] Moreover, PROTAC approach abrogates all enzymatic, structural, and scaffolding functions of POI simultaneously, resulting in higher drug potency.[40] Since the first PROTAC-based degrader from Arvinas Therapeutics entered clinical trial in 2019, FDA has approved 12 additional candidates from the same class for trials in the last two years,[48] heralding a new era of drug discovery for PROTAC.

Benzamide DC541 (Figure 1B) was recently developed as a peptidomimetic inhibitor targeting NTMT1 and represents one of the best cell-permeable inhibitors thus far, exhibiting cellular IC_{50} at ~30 and >100 μM for HT29 and HCT116, respectively.[33] Chemical conversion of a known inhibitor into PROTAC-based degrader has been demonstrated to be an effective strategy for improved cellular potency.[38, 49–53] Therefore, we decided to employ this approach to develop NTMT1 degraders in hope for enhanced cellular and therapeutic activities.

To test the feasibility of our approach, we first performed a SwissDock study of compound **14** (Figure 1B), which is a carboxyl analog of DC541, with NTMT1 based on the known X-ray crystal structure of the enzyme complexed with DC113 (PDB 7K3D).[33] As shown in Figure 1C, while the naphthyl group is deeply buried in the active site, the *ortho*-carboxylic acid group protrudes out of the pocket and is solvent-exposed. Compound **14** was overlaid with DC113, which were found to be highly superimposable (Figure 1D). Thus, the PROTAC molecule could be prepared by linking an E3 ligase ligand to the carboxyl group in **14** via an ethylene glycol (EG) linker. Two types of E3 ligands, including cereblon (CRBN) and VHL ligands, are commonly used for PROTACs.[54] The latter was selected for our study because (1) CRBN-based PROTACs may cause the resistance of cancer cells through inactivation of their *crbn* gene;[55] (2) both the VHL ligand and **14** (or DC541) are peptidomimetic compounds. We hypothesized that the resulting PROTAC molecules might have improved cellular potency due to increased hydrophobicity originated from the formation of intramolecular hydrogen bonds present in peptides,[56–57] which are known to facilitate compounds' penetration into cell membrane via passive diffusion.[56–57]

Author Manuscript Author Manuscript Author Manuscript Author Manuscript

Degraders **1–3** with various EG linker lengths were prepared using the synthetic routes outlined in Scheme 1. While DC541 was reported to be produced in a linear fashion,[33] we decided to pursue a parallel synthesis, as the latter allowed us to obtain DC541 in sufficient amounts in high yields. Briefly, intermediate **7** was obtained from commercially available **5** and **6** using phosphorus oxychloride as an efficient coupling reagent. Intermediate **11** was produced from **9** and **10** using standard amide coupling followed by basic hydrolysis. A second coupling between amine **8** and acid **11** gave intermediate **12**, which was hydrolyzed under a basic condition to produce acid **13A**. Finally, compound **14** and its amide analog DC541 were obtained in 8 steps in total yields of 54% and 39%, respectively.

Compounds **15A-D** consisting of a VHL ligand (*trans* hydroxyproline) or negative control (*cis* hydroxyproline) and different lengths of EG linkers were prepared according to the procedures (Scheme S1) modified from previous reports.[58–59] After they were converted into amines by Pd/C-catalyzed hydrogenation followed by a standard amide coupling with **13A**, compounds **16A-D** were produced. Subsequent acidic removal of Boc protection group afforded degraders **1–3** (containing *trans*-VHL) and negative control/inhibitor **4** (containing *cis*-VHL) in total yields of 30–33%. All compounds subjected to cellular evaluations were determined to be >96% pure by HPLC (Figure S1) and stable in cell culture medium for >72 h (Figure S2).

Inhibition of NTMT1 in vitro.

We first evaluated the effects of synthesized compounds on inhibiting the activity of purified NTMT1. Assays were performed by monitoring at λ_{260} for the release of SAH using HPLC. As summarized in Figures 2 and S3, compounds **1–4** display similar inhibitory effects on NTMT1 at IC_{50} ~2.00 μM, which is ~4- and ~2-fold more potent than the parent inhibitor **14** (IC_{50} = 9.18 μM) and its amide analog DC541 (IC_{50} = 4.38 μM), respectively. The increase in potency relative to both parent inhibitors is attributed to the presence of linker and VHL ligand in compounds **1–4**, which may provide additional binding affinities with NTMT1. As expected, the linker length had a negligible impact on IC_{50} as linkers are not involved in direct inhibition.

Degradation of NTMT1 in vitro.

We next assessed the degradation effects of **1–3** on NTMT1 in human colorectal carcinoma cell lines HCT116 and HT29. We were pleased to find out that all degraders could reduce NTMT1 protein level in a dose-dependent manner (Figures 3A–B and S4). In contrast to *in vitro* inhibition assays, linker length played a significant role on degradation efficacy. Degrader **1** containing one EG linker displayed the highest potency with DC_{50} values at 7.53 and 18.1 μM in HCT116 and HT29, respectively (Figure 3B). The maximal degradation (D_{max}) with **1** was determined to be > 90% for both cell lines. Compared with the reported cellular IC_{50} values of DC541,[33] which were >100 and ~30 μM for HCT116 and HT29, respectively, degrader **1** showed significantly improved cellular potency due to deployment of PROTAC technology. Longer linkers of two and four EG units present in degraders **2** and **3**, respectively, greatly reduced their effects of degradation (Figure S4). As summarized in Figure 3C, degraders **2** and **3** have DC_{50} values at 79.7 and 66.4 μM, respectively, in HCT116, which are at least ~9 fold less potent than degrader **1**. In HT29, degraders **2** and **3**

Author Manuscript Author Manuscript Author Manuscript Author Manuscript

displayed similar potency with DC_{50} at 53.7 μM, which is ~3-time less potent than degrader **1**. Altogether, these results indicate that the PROTAC-based degraders exhibit improved cellular potency compared with their parent inhibitor DC541, possibly due to the enhanced hydrophobicity.

To demonstrate that the observed NTMT1 degradation was due to VHL E3 ligase activity, a negative control experiment was carried out with inhibitor **4** containing *cis*-VHL, which is known to abolish E3 ligase-recruiting activity.[60] As expected, inhibitor **4** was unable to reduce NTMT1 levels relative to the DMSO control in both HCT116 and HT29 cells (Figure 3D), suggesting that VHL is responsible for the observed PROTAC effect of degrader **1**. Furthermore, degradation was completely abolished when HCT116 was pre-treated with 1 μM MG-132 (proteosome inhibitor) or 1 μM MLN4924 (NEDD8-activating enzyme inhibitor), indicating that the PROTAC-based degrader **1** depends on the proteasome and ubiquitination cascade (i.e., neddylation of CUL2) for its action (Figure 3E).

To further demonstrate NTMT1 degradation induced by degrader **1**, an enhanced green fluorescence protein (eGFP) was fused to C-terminus of NTMT1. HCT116 cells were transiently transfected with the plasmid expressing the fusion protein using Lipofectomine 3000 (ThermoFisher). After 24 h of transfection, cells were treated with DMSO (control) or 100 μM degrader **1** for another 24 h and then inspected by fluorescence microscopy. As illustrated in Figure 3E, most fluorescence signals were lost in cells treated with degrader **1**, consistent with our results obtained from Western blots (Figures 3A). Additional controls were also performed with the plasmid expressing only eGFP, in which cells treated with DMSO or degrader **1** did not show obvious reduction of fluorescence (Figure S5), demonstrating that NTMT1 was the protein targeted for degradation by our degrader.

Characterization of degrader 1.

Since degrader **1** was the most active compound in our series toward NTMT1 degradation, we decided to further characterize its pharmacokinetic properties, selectivity, and cytotoxicity. NTMT1 degradation was also studied in a time-dependent manner. It was found that the kinetics of protein degradation by degrader **1** was faster in HCT116 than in HT29 (Figure 4A). When HCT116 cells were treated with 50 μM degrader **1**, > 60% NTMT1 was degraded within 3 h and almost completely depleted within 24 h. However, under the same condition, a pronounced change of NTMT1 levels was not observed until 6 h and > 90% degradation were achieved within 24 h for HT29.

It has been reported that the PROTAC-induced protein degradation does not impair re-synthesis of the protein.[39] We therefore also investigated whether the NTMT1 degradation induced by degrader **1** could be rescued by using a washout method. To this end, both cell lines were treated with **1** at 50 μM for 24 h followed by washing it out. Recovery of the NTMT1 protein level was then monitored by Western blots. It was found that the washout led to NTMT1 recovery within 20 h for both cell lines (Figure 4B), highlighting that the protein silencing via PROTAC is reversible.[61] This is in a stark contrast with some other protein silencing methods such as CRISPR/Cas9 that are irreversible.[61]

Author Manuscript Author Manuscript Author Manuscript Author Manuscript

Our degrader **1** was developed based on inhibitor DC541,[33] which was originally modified from BM30.[34] While both inhibitors exhibited excellent selectivity toward NTMT1 versus other types of human methyltransferases,[33–34] their selectivity toward NTMT1 and NTMT2 are likely to be low, as these highly homologous enzymes have almost identical 3D structures and display the same N-terminal (M)XPK motif sequence for their substrate preference.[62–65] In fact, BM30 has been reported to be a nonselective inhibitor toward NTMT1 and NTMT2.[34] We decided to investigate the selectivity of degrader **1**. As shown in Figure 4C, although degrader **1** exhibits the ability to deplete NTMT1 (MW 25.4 KDa) in both HCT116 and HT29 in a dose-dependent manner, it cannot induce degradation of NTMT2 (MW 32.4 KDa), indicating that degrader **1** is highly selective toward NTMT1. This finding is significant because, for the first time, PROTAC offers a way to target cellular NTMT1 specifically. Access to such probes will allow us to study the relationship of NTMT1 and NTMT2, which remains enigmatic and challenging.

Cytotoxicity of degrader **1** and inhibitor **4** was evaluated on both HCT116 and HT29 using a WST-8 assay. Cells were treated with both compounds for 24 h and then tested for their viability using WST-8 in the presence of 1-methoxy PMS.[66] No significant cytotoxicity was observed in either cell line with degrader **1** or inhibitor **4** up to 64 μM (Figure 4D).

Antiproliferative effect of degrader 1.

After degrader **1** was identified to effectively reduce cellular NTMT1 levels, we evaluated its role in proliferation of HCT116 in 2D and 3D culture environment along with the negative control/inhibitor **4**. As illustrated in Figure 5A, both compounds inhibited HCT116 proliferation in a dose-dependent manner. After treating cells with both compounds at 64 μM for 72 h, DNA quantifications revealed that degrader **1** and control/inhibitor **4** inhibited cell proliferation by ~47% and ~22%, respectively, relative to the DMSO control. This demonstrates that inhibition of N-terminal methylation induced by control/inhibitor **4** has an antiproliferative effect on human colorectal carcinoma cells in 2D environment, which becomes much more significant upon NTMT1 degradation induced by degrader **1**. The latter observation agrees well with the reported growth defects found in *ntmt1* KO HCT116 cells.[23] To study the off-target potential of the compounds due to their relatively high concentrations, the same experiments were repeated with *ntmt1* KO HCT116 cells (Figure S6). As expected, neither compound displayed an antiproliferative effect (Figure 5B) on the KO cells, suggesting that degrader **1** and inhibitor **4** target only NTMT1 in HCT116.

While cell-based assays on monolayer surfaces (2D) have been widely adapted for compound evaluation, there are increasing concerns to its questionable correlation with animal models.[67] In human body, almost all tissue cells reside in an extracellular matrix (ECM), providing a 3D framework rather than flat surface representative of a 2D culture system.[68] Such difference has been known to affect a myriad of cellular functions such as cell morphology, cell-cell interaction, and cellular processes like proliferation, apoptosis, differentiation, migration, gene expression, and drug sensitivity.[69] Therefore, the antiproliferative effects of degrader **1** and inhibitor **4** were also evaluated in 3D environment to mimic complex situation of tumor growth in human. We first tested the growth of HCT116 tumor spheroids in the presence of these two compounds over a period of 12

Author Manuscript Author Manuscript Author Manuscript Author Manuscript

days using a 96-well plate with ultralow surface attachment. After 3-day incubation (day 0), these spheroids were treated with DMSO or compounds at 32 and 64 μM every three days. Pictures were then taken on day 0, 3, 6, 9, and 12 (Figure 5C). Growth of spheroids was monitored by measuring their diameters, which were then compared to day 0 (Figure 5D and Figure S7). It was observed that the tumor spheroids treated with both compounds were significantly smaller than the control treated with DMSO. A 12-day exposure to degrader **1** and negative control/inhibitor **4** at 64 μM inhibited the spheroid sizes by 62%, and 32%, respectively, relative to the DMSO control (Figures 5D), replicating their 2D antiproliferative effects in 3D environment.

PGmatrix-Spheroid (PG-S, PepGel LLC) is a peptide hydrogel that can provide a number of desirable cellular microenvironment characteristics: 3D spatial support for cell growth; porosities for cell migration; and facile transportation of gases, nutrients, wastes, and other soluble materials.[70] Due to its amino acid composition, PGS is thought to be structurally and mechanically similar to ECM.[70] Thus, PGS is considered as an advanced *in vitro* tumor spheroid model with real physiological relevance.[70–71] Therefore, we repeated the aforementioned experiments with the PGS for a period of 3 days. Subsequently, cells were subjected to acridine orange (AO)−propidium iodide (PI) assay followed by automated cell counting. It was found that the number of cells decreased as the compound concentration increased (Figure 5E). Like observations described above, degrader **1** displayed an enhanced antiproliferative effect relative to the negative control/inhibitor **4**, as the number of cells fell to 68% and 78% of the DMSO control for samples treated with **1** and **4**, respectively, at 64 μM. Percentages of live cells (viability) were always >92% regardless of compound concentrations up to 64 μM (Figure 5E). Altogether, these results demonstrate that, compared with NTMT1 inhibition, NTMT1 degradation has an enhanced antiproliferative effect on HCT116 in both 2D and 3D environment with marginal cytotoxicity, which is consistent with previous report that *ntmt1* gene knockout in HCT116 resulted in pronounced defects in cell proliferation.[23]

N-terminal methylation catalyzed by NTMT1 is known to play important roles in cell mitosis and DNA repair.[15–16] The observed inhibitory activity of degrader **1** toward NTMT1 suggests that this compound could lead to cell cycle arrest and result in the observed antiproliferative effect. To evaluate it, HCT116 cells were treated with the degrader **1** for 3 days before analyzed by flow cytometry. It was found that degrader **1** induced cell cycle arrest at G0/G1 phase in a dose-dependent manner (Figure 5F and Figure S8). Proportion of the cells at G0/G1 phase was 65% for the DMSO control group, which increased to 71% upon treatment with the degrader **1** at 64 μM for 3 days along with the concurrent reduction of S phase cells. These results indicate that degrader **1** induces inhibition of cell cycle progression, which explains its antiproliferative effect on colorectal carcinoma HCT116 cells.

Increased calreticulin (CALR) expression induced by degrader 1.

To date, cellular mechanism and physiological function of NTMT1 remain elusive. While NTMT1 has been suggested to be an oncogene and potential drug target for colorectal cancer,[23, 26–28] its exact role is still unknown and requires extensive study. To this end,

Author Manuscript Author Manuscript Author Manuscript Author Manuscript

we decided to investigate the global change of protein expression upon NTMT1 depletion induced by degrader **1** using MS-based label-free quantitative global proteomic analysis. To eliminate proteins that would undergo expression level changes simply due to NTMT1 inhibition, compound **4** was used as a control instead of DMSO because **4** would inhibit, but not degrade NTMT1. Thus, lysates of the HCT116 cells treated with degrader **1** or control **4** at 25 μM for 24 h were subject to on-column trypsin digestion followed by liquid chromatography-mass spectrometry (LC/MS). Data analysis using Progenesis QI for Proteomics (Waters) identified 1013 and 813 proteins undergoing up- and down-regulation induced by degrader **1**, respectively (Excel file in Supplementary Data). As illustrated in the volcano plot (Figure 6A), a total of 127 proteins display fold-change ≥ 1.5 with statistical significance ≤ 0.001 (two-sample t-test). A further ranking based on the number of unique peptides detected (≥ 4) gave 5 hits, in which NTMT1 (labeled as a blue dot in Figure 6A) was the only protein underwent downregulation in the presence of degrader **1**. Four proteins (labeled as red dots in Figure 6A) were found to have increased expression levels, in which CALR displayed the highest fold changes and thus, caught our attention. CALR is an essential Ca^{2+}-binding endoplasmic reticulum (ER)-resident protein that regulates a variety of cellular processes such as chaperon activity, Ca^{2+} homeostasis, integrin signaling, folding and oligomerization of gastrointestinal mucin synthesis, and loading of cellular antigens onto MHC-I molecules.[72] More importantly, CALR is also an indispensable immunogenic cell death (ICD) signal protein that triggers phagocytosis of cells upon its translocation from ER lumen to the cell surface.[73–74] Accumulating clinical data has shown that CALR can elicit antitumor immunogenic responses upon T-cell infiltration. A clinical trial based on this is currently ongoing.[75] Thus, expression level of CALR can be considered as a prognostic/predictive factor of cancers.[73, 76–77] Specifically, robust CALR expression detected in biopsy has been linked to a high survival rate and viewed as a good prognostic indicator for patients with colorectal cancer.[78–80]

Our global proteomic analysis revealed that the level of CALR expression was 1.6-time higher in the sample treated with degrader **1** than in the control treated with inhibitor **4**. To further confirm it, the level of CALR expression was also quantified by Western blot using anti-CALR antibody. As illustrated in Figure 6B, NTMT1 was almost depleted upon treatment with degrader **1** at 25 μM for 24 h. Under the same condition, expression of CALR was increased to 1.5 and 1.1 folds relative to the DMSO control for degrader **1** and inhibitor **4**, respectively. This is translated into the fact that CALR expression in the presence of degrader **1** is ~1.4-fold higher than that in the presence of inhibitor **4**, which is consistent with the result from proteomic analysis. Altogether, our study has demonstrated that the ICD signal protein CALR is upregulated upon NTMT1 degradation, which may offer a potential therapeutic strategy for treatment of colorectal cancer. Further investigation of the pathways involving NTMT1 and CALR is currently in progress.

CONCLUSION

Although protein N-terminal methylation catalyzed by NTMT1 is widely present in eukaryotic cells and has been shown to play pivotal regulatory roles in various biological processes,[14–15, 17–18, 20–21] its cellular mechanisms remain elusive due to the inaccessibility

Author Manuscript Author Manuscript Author Manuscript Author Manuscript

to chemical probes that can effectively penetrate cell membrane. Through a brief SAR study, we developed the first-in-class, PROTAC-based, NTMT1-selective degrader **1**, which is a bifunctional molecule consisting of a VHL-recruiting ligand, NTMT1 inhibitor DC541, and EG linker. Degrader **1** could effectively reduce NTMT1 level in dose- and time-dependent manners in colorectal carcinoma cell lines HCT116 and HT29. Degrader **1** was found to have significant higher cellular potency than its parent inhibitor DC541 in HCT116 and HT29. Thus, it represents the first cellular probe that can be employed to selectively study N-terminal methylation catalyzed by NTMT1. While degrader **1** exhibited marginal cytotoxicity, it could inhibit the proliferation of HCT116 in 2D and 3D culture environment, resulting from its cell cycle arrested at G0/G1 phase. Label-free quantitative global proteomic analysis indicated that degrader **1** could induce expression level changes of more than 1800 proteins in HCT116. Among them, expression of an ICD signal protein, CALR, increased by ~50%. Upregulation of CALR has been clinically linked to a high survival rate of patients with colorectal cancer,[78–80] which is attributed to CALR-mediated antitumor immunogenic responses, suggesting that NTMT1-directed PROTACs reported herein may also offer a new drug discovery modality for NTMT1-related oncology and diseases.

EXPERIMENTAL SECTION

Chemistry.

General Information—All chemical and biochemical reagents were purchased at the highest purity grade. Unless otherwise specified, all solvents were anhydrous, and all chemical syntheses were performed under argon atmosphere. Silica gel (ZEOprep® 60 HYD, 40–63 μm) was used for flash column chromatography. Thin layer chromatography (TLC) was performed using 60 mesh silica gel plates and visualized either at short wavelength UV light (254 nm) or basic $KMnO_4$ staining. Nuclear magnetic resonance (NMR) spectra were recorded on a Varian 400 MHz spectrometer. Chemical shifts of proton (^{1}H NMR) and carbon (^{13}C NMR) were reported in parts per million (ppm) referenced to $CDCl_3$: δ = 7.26 ppm (^{1}H) and 77.00 ppm (^{13}C) or CD_3OD: δ = 3.31 ppm (^{1}H) and 49.00 ppm (^{13}C). The following abbreviations were used for spin multiplicity: s (singlet), d (doublet), t (triplet), q (quartet), dd (doublet of doublet), m (multiplet), and br (broad). Coupling constants were reported in hertz (Hz). All samples for HPLC and mass spectrometry (MS) were filtered using either a 0.2 μm PTFE syringe or centrifugal filter to remove particles before injection. HPLC was performed on a Waters Breeze 2 system consisting of 1525 pump and 2998 photodiode array detector. High-resolution MS (HRMS) and LC/MS were recorded on a Waters ACQUITY M-class UPLC coupled with Waters Xevo G2-XS QTof mass spectrometer that is equipped with a NanoLockSpray exact mass ionization source. All compounds subjected to cellular evaluation are >96% pure by HPLC.

Methyl(S)-2-(2-((((9H-fluoren-9-yl)methoxy)carbonyl)amino)-6-((tertbutoxycarbonyl)amino)hexanamido)benzoate 7.[81]—Fmoc-Lys(Boc)-OH **5** (4.69 g, 10.0 mmol) and methyl 2-aminobenzoate **6** (1.52 g, 10.0 mmol) were dissolved in 30 mL dry pyridine. The yellowish clear solution was cooled to −15°C and added phosphorus oxychloride (1.12 mL, 12.0 mmol) dropwise with vigorous stirring. The mixture became dark red and turbid during addition. Color of the suspension slowly

Author Manuscript Author Manuscript Author Manuscript Author Manuscript

changed to orange after the addition was done. The reaction was then kept stirring until its completion as monitored by TLC (~30 min). After the reaction mixture was quenched with ice/water (100 mL), the aqueous layer was separated and extracted with EtOAc (50 mL × 4). The organic layer and extractions were combined, washed with saturated $NaHCO_3$ (30 mL × 3) and brine (30 mL × 3) sequentially, dried with anhydrous Na_2SO_4, and concentrated under vacuum. The residue was co-evaporated with toluene twice under 50 °C. Crude product was purified by silica gel chromatography (Hexane/EtOAc = 2/1) to give **7** as white solid (5.40 g, 90%); R_f = 0.7, Hexane/EtOAc = 2/1; ^{1}H NMR (400 MHz, $CDCl_3$) δ 11.60 (s, 1H), 8.71 (d, J = 8.0 Hz, 1H), 8.02 (dd, J = 8.0, 1.4 Hz, 1H), 7.76 (d, J = 7.6 Hz, 2H), 7.70 (d, J = 7.6 Hz, 1H), 7.65 (d, J = 7.6 Hz, 1H), 7.55 (t, J = 7.6 Hz, 1H), 7.39 (t, J = 7.6 Hz, 2H), 7.34–7.26 (m, 2H), 7.10 (t, J = 7.6 Hz, 1H), 5.72 (br, 1H), 4.62 (br, 1H), 4.58–4.49 (m, 1H), 4.45–4.36 (m, 1H), 4.34–4.26 (m, 2H), 3.79 (s, 3H), 3.20–3.06 (m, 2H), 2.06–1.95 (m, 1H), 1.92–1.78 (m, 1H), 1.61–1.45 (m, 4H), 1.42 (s, 9H); ^{13}C NMR (101 MHz, $CDCl_3$) δ 170.8, 168.5, 156.2, 144.1, 143.7, 141.2, 141.2, 140.9, 134.6, 130.8, 127.6, 127.0, 127.0, 125.4, 125.2, 122.9, 120.4, 119.9, 115.3, 79.2, 77.2, 67.2, 56.3, 52.3, 47.2, 39.8, 32.2, 29.7, 28.4, 22.4; HRMS: m/z $[M+H]^+$ Calcd. for $C_{34}H_{40}N_3O_7$, 602.2866 Found: 602.2845.

Methyl (S)-2-(2-amino-6-((tert-butoxycarbonyl)amino)hexanamido)benzoate 8.—Compound **7** (1.00 g, 1.66 mmol) was dissolved in a solution of 20% piperidine in DMF (10 mL). The mixture was stirred at r.t. for 20 min followed by sequential additions of Et_2O (30 mL) and brine (30 mL). The aqueous layer was separated and extracted with Et_2O (50 mL × 3). The organic layer and extractions were combined, dried with anhydrous Na_2SO_4, and concentrated under vacuum. After the remaining DMF was removed by azeotropic distillation with toluene, the residue was quickly purified by a short silica gel column eluted with hexane/acetone (3/1) to yield crude amine **8** as yellow oil (605 mg, 96%).

(2-(naphthalen-1-yl)acetyl)-L-proline 11.—A solution of sodium 2-(napthalen-1-yl)acetate **10** (4.00 g, 19.2 mmol), EDCI (4.42 g, 23.1 mmol), and HOAT (1.57 g, 11.5 mmol) dissolved in DMF (100 mL) was stirred for 5 min and then injected with *N*-methylmorpholine (NMM, 5.27 mL, 48.0 mmol). The reaction mixture was stirred for another 15 min and methyl *L*-prolinate hydrochloride **9** (3.82 g, 23.1 mmol) was added. The mixture was kept stirring overnight at r.t. Upon completion of the reaction monitored by TLC, 2M HCl (50 mL) solution was added into the mixture followed by extraction with Et_2O (200 mL × 4). The organic extractions were combined, dried with anhydrous Na_2SO_4, and concentrated under vacuum. After the remaining DMF was removed by azeotropic distillation with toluene, the residue was quickly purified by a short silica gel column eluted with hexane/EtOAc (from 1.5/1 to 1/1) to give crude product as white solid (4.80 g).

The crude product (2.17 g, 7.30 mmol) was dissolved in 50 mL THF and 100 mL H_2O. The mixture was then cooled in ice bath, added slowly with NaOH (0.88 g, 22 mmol), and kept stirring overnight. After the solvent was removed under vacuum, pH of the solution was adjusted to ~4 using 12 M HCl. The white solid formed during pH adjustment was collected via filtration and re-dissolved in 50 mL CH_2Cl_2. The organic layer was dried with anhydrous Na_2SO_4 and concentrated under vacuum to afford **11** as white foam (1.71 g, 70% for two steps); R_f = 0.1, CH_2Cl_2/MeOH = 20/1; ^{1}H NMR (400 MHz, $CDCl_3$) δ 7.92 (d, *J*

Author Manuscript Author Manuscript Author Manuscript Author Manuscript

= 8.4 Hz, 1H), 7.90–7.85 (m, 1H), 7.80 (d, *J* = 8.0 Hz, 1H), 7.57–7.47 (m, 2H), 7.46–7.41 (m, 1H), 7.38 (d, *J* = 6.8 Hz, 1H), 4.70–4.60 (m, 1H), 4.19 (d, J = 15.6 Hz, 1H), 4.14 (d, J = 15.6 Hz, 1H), 3.69–3.58 (m, 1H), 3.57–3.45 (m, 1H), 2.44–2.33 (m, 1H), 2.13–1.93 (m, 3H); ^{13}C NMR (101 MHz, $CDCl_3$) δ 172.9, 172.8, 133.8, 132.0, 129.9, 128.8, 128.1, 126.8, 126.5, 125.9, 125.5, 123.4, 60.1, 48.1, 39.3, 27.6, 24.9; HRMS: *m/z* $[M+H]^+$ Calcd. for $C_{17}H_{18}NO_3$, 284.1287 Found: 284.1300.

Methyl 2-((S)-6-((tert-butoxycarbonyl)amino)-2-((S)-1-(2-(naphthalen-1-yl)acetyl)pyrrolidine-2-carboxamido)hexanamido)benzoate 12.—A mixture of amine **8** (1.22 g, 3.22 mmol) and NMM (406 μL, 3.70 mmol) in DMF (5 mL) was added to a solution of **11** (700 mg, 2.47 mmol), EDCI (714 mg, 3.70 mmol) and HOAT (504 mg, 3.70 mmol) in DMF (35 mL). After the reaction was stirred at r.t. overnight, EtOAc (50 mL) and brine (50 mL) were added sequentially to the mixture. The aqueous layer was separated and extracted with EtOAc (50 mL × 2). The organic layer and extractions were combined, dried with anhydrous Na_2SO_4, and concentrated under vacuum. After the remaining DMF was removed by azeotropic distillation with toluene, the residue was purified by silica gel chromatography eluted with CH_2Cl_2/EtOAc (from 4/1 to 2/1) to give **12** as white foam (1.50 g, 94%); R_f = 0.7, CH_2Cl_2/MeOH = 10/1; ^{1}H NMR (400 MHz, $CDCl_3$) δ 11.42 (s, 1H), 8.57 (dd, J = 8.4, 1.2 Hz, 1H), 7.87 (dd, J = 8.0, 1.2 Hz, 1H), 7.83 (d, J = 8.4 Hz, 1H), 7.78–7.72 (m, 1H), 7.67 (d, J = 8.4 Hz, 1H), 7.59 (d, J = 7.6 Hz, 1H), 7.45–7.34 (m, 3H), 7.34–7.29 (m, 1H), 7.25 (d, J = 6.8 Hz, 1H), 6.95 (t, J = 8.0 Hz, 1H), 4.76 (d, J = 6.1 Hz, 1H), 4.43–4.33 (m, 1H), 4.09 (d, J = 16.0 Hz, 1H), 4.00 (d, J = 16.0 Hz, 1H), 3.76 (s, 3H), 3.65–3.54 (m, 1H), 3.49–3.37 (m, 1H), 2.86–2.75 (m, 1H), 2.73–2.62 (m, 1H), 2.44–2.29 (m, 1H), 2.20–2.03 (m, 1H), 1.94–1.70 (m, 3H), 1.59–1.45 (m, 1H), 1.26 (s, 9H), 1.25–1.06 (m, 4H); ^{13}C NMR (101 MHz, $CDCl_3$) δ 171.6, 171.5, 170.6, 168.4, 155.9, 140.9, 134.5, 133.8, 132.0, 130.7, 130.6, 128.8, 127.9, 126.9, 126.3, 125.8, 125.5, 123.5, 122.7, 120.2, 115.2, 78.7, 77.20, 60.1, 54.5, 52.2, 48.0, 39.5, 31.3, 28.3, 29.0, 27.1, 25.2, 22.3; HRMS: m/z $[M+H]^+$ Calcd. for $C_{36}H_{45}N_4O_7$, 645.3288 Found: 645.3300.

2-((S)-6-((tert-butoxycarbonyl)amino)-2-((S)-1-(2-(naphthalen-2-yl)acetyl)pyrrolidine-2-carboxamido)hexanamido)benzoic acid 13A.—To a solution of **12** (900 mg, 1.40 mmol) in THF (20 mL) was added H_2O (40 mL) and 1M NaOH (7.00 mL, 7.00 mmol). The mixture was stirred overnight at r.t. After the reaction was complete, it was quenched with 1 M HCl (8 mL). The mixture was then extracted with EtOAc (15 mL × 3). The combined extractions were dried with anhydrous Na_2SO_4 and concentrated under vacuum to afford acid **13A** as white solid (854 mg, 97% crude yield), which was used directly for the next step without further purification.

tert-butyl ((S)-6-((2-carbamoylphenyl)amino)-5-((S)-1-(2-(naphthalen-1-yl)acetyl)pyrrolidine-2-carboxamido)-6-oxohexyl)carbamate 13B.—DIPEA (110 μL, 0.632 mmol) was added to a mixture of **13A** (100 mg, 0.158 mmol), NH_4Cl (68 mg, 1.27 mmol), EDCI (61 mg, 0.317 mmol), and HOAT (43 mg, 0.317 mmol) in DMF (10 mL). The reaction was stirred at 80°C for 5 h. EtOAc (50 mL) and brine (20 mL) were added to the mixture sequentially. The aqueous layer was separated and extracted with EtOAc (10 mL × 5). The organic layer and extractions were combined, dried with anhydrous Na_2SO_4,

Author Manuscript Author Manuscript Author Manuscript Author Manuscript

and concentrated under vacuum. After the remaining DMF was removed by azeotropic distillation with toluene, the residue was purified by silica gel chromatography eluted with CH_2Cl_2/MeOH (from 40/1 to 20/1) to give **13B** as white foam (80 mg, 80%); R_f = 0.3, CH_2Cl_2/MeOH = 20/1; ^{1}H NMR (400 MHz, $CDCl_3$) δ 11.79 (s, 1H), 8.61 (d, J = 8.4 Hz, 1H), 7.94 (d, J = 8.0 Hz, 1H), 7.91 – 7.82 (m, 2H), 7.78 (d, J = 8.2 Hz, 1H), 7.56 – 7.33 (m, 6H), 7.00 (t, J = 7.3 Hz, 1H), 6.69 (s, 2H), 4.85 (d, J = 5.3 Hz, 1H), 4.54 – 4.43 (m, 1H), 4.26 – 4.05 (m, 2H), 3.73 (d, J = 11.4 Hz, 1H), 3.51 (q, J = 11.8, 9.9 Hz, 1H), 2.86 (d, J = 10.4 Hz, 1H), 2.74 (s, 1H), 2.31 (d, J = 11.5 Hz, 1H), 2.20 (d, J = 18.6 Hz, 1H), 2.03 – 1.77 (m, 3H), 1.58 – 1.45 (m, 1H), 1.41 (s, 9H), 1.27 (d, J = 11.1 Hz, 4H); ^{13}C NMR (101 MHz, $CDCl_3$) δ 172.2, 171.8, 171.1, 170.8, 156.1, 139.7, 133.8, 133.2, 132.1, 130.7, 128.8, 127.9, 127.4, 127.0, 126.4, 125.8, 125.5, 123.7, 122.9, 121.2, 118.9, 79.0, 60.3, 54.6, 48.1, 39.7, 31.7, 29.2, 28.4, 28.1, 25.2, 22.9. HRMS: m/z $[M+H]^+$ Calcd. for $C_{35}H_{44}N_5O_6$, 630.3292 Found: 630.3307.

2-((S)-6-amino-2-((S)-1-(2-(naphthalen-1-yl)acetyl)-pyrrolidine-2-carboxamido)hexanamido)benzoic acid 14.—A solution of acid **13A** (100 mg, 0.160 mmol) in CH_2Cl_2 (3 mL) was added 4M HCl in dioxane (2 mL) at 0 °C. Then the reaction was slowly warmed up to r.t. in 1 h. Solvent was removed under vacuum and the residue was purified by silica gel chromatography eluted with CH_2Cl_2/0.5 M NH_3 in MeOH (from 20:1 to 5:1) to give product **14** as white foam (84.0 mg, 99%); R_f = 0.6, CH_2Cl_2/MeOH = 5/1; ^{1}H NMR (400 MHz, CD_3OD) *δ* 8.50 (d, *J* = 8.0 Hz, 1H), 8.04 (dd, *J* = 8.0, 1.6 Hz, 1H), 7.88 (dd, *J* = 14.0, 8.0 Hz, 2H), 7.78 (d, *J* = 8.0 Hz, 1H), 7.57–7.31 (m, 5H), 7.05 (t, *J* = 7.6 Hz, 1H), 4.57–4.50 (m, 1H), 4.49–4.41 (m, 1H), 4.17 (d, *J* = 16.8 Hz, 1H), 4.10 (d, *J* = 16.4 Hz, 1H), 3.81–3.60 (m, 2H), 2.62 (dt, *J* = 12.4, 7.2 Hz, 1H), 2.45 (dt, *J* = 12.8, 6.0 Hz, 1H), 2.35–2.28 (m, 1H), 2.21–2.07 (m, 2H), 2.03–1.89 (m, 2H), 1.76–1.65 (m, 1H), 1.53–1.38 (m, 4H); ^{13}C NMR (101 MHz, CD_3OD) *δ* 175.1, 174.4, 172.5, 172.3, 140.8, 135.2, 133.6, 132.7, 132.4, 132.2, 129.7, 128.9, 128.5, 127.4, 126.9, 126.6, 125.2, 123.8, 120.5, 61.7, 55.5, 40.4, 40.0, 32.2, 30.8, 27.2, 26.0, 23.4; HRMS: *m/z* $[M+H]^+$ Calcd. for $C_{30}H_{35}N_4O_5$, 531.2607 Found: 531.2626.

(S)-N-((S)-6-amino-1-((2-carbamoylphenyl)amino)-1-oxohexan-2-yl)-1-(2-(naphthalen-1-yl)acetyl)pyrrolidine-2-carboxamide DC541.—The reaction was performed in the same way as **14** starting with **13B** (65 mg, 0.103 mmol), 4M HCl in dioxane (1.3 mL) to give **DC541** as white foam (48 mg, 88%); R_f = 0.5, CH_2Cl_2/MeOH = 5/1; ^{1}H NMR (400 MHz, CD_3OD) δ 8.46 (d, *J* = 8.3 Hz, 1H), 7.91 (t, *J* = 7.1 Hz, 2H), 7.83 (d, *J* = 7.8 Hz, 1H), 7.78 (d, *J* = 7.2 Hz, 1H), 7.58 – 7.39 (m, 5H), 7.16 (t, *J* = 7.4 Hz, 1H), 4.58 (dd, *J* = 8.0, 5.1 Hz, 1H), 4.43 (dd, *J* = 10.7, 4.0 Hz, 1H), 4.31 – 4.09 (m, 2H), 3.92 – 3.71 (m, 2H), 2.64 (dt, *J* = 12.7, 6.5 Hz, 1H), 2.43 (dq, *J* = 15.8, 8.0 Hz, 2H), 2.31 (dt, *J* = 12.9, 6.4 Hz, 1H), 2.23 (s, 1H), 2.11 – 1.91 (m, 2H), 1.82 – 1.69 (m, 1H), 1.53 – 1.36 (m, 4H); ^{13}C NMR (101 MHz, CD_3OD) δ 175.7, 173.0, 172.7, 140.0, 135.2, 133.6, 133.4 132.8, 129.7, 129.5, 129.0, 128.6, 127.4, 126.9, 126.6, 125.2, 124.6, 122.2, 122.1, 61.9, 55.3, 40.5, 40.0, 31.8, 30.8, 27.1, 26.2, 23.5; HRMS: m/z $[M+H]^+$ Calcd. for $C_{30}H_{36}N_5O_4$, 530.2767 Found: 530.2760.

Author Manuscript Author Manuscript Author Manuscript Author Manuscript

tert-Butyl ((S)-6-((2-((2-(2-(((2S,4R)-4-hydroxy-1-((S)-3-methyl-2-(1-oxoisoindolin-2-yl)butanoyl)pyrrolidine-2-carboxamido)methyl)-5-(4-methylthiazol-5-yl)phenoxy)ethyl)carbamoyl)phenyl)amino)-5-((S)-1-(2-(naphthalen-1-yl)acetyl)pyrrolidine-2-carboxamido)-6-oxohexyl)carbamate

16A.—A mixture of **15A** (350 mg, 0.576 mmol) and 10% Pd/C (175 mg) in EtOH (12 mL) was stirred under H_2 at r.t. for 5 h. Pd/C was filtered, and the filtrate was concentrated under vacuum to yield amine, which was used directly for the next step without further purification.

A solution of **13A** (465 mg, 0.739 mmol), EDCI (163 mg, 0.852 mmol), HOAT (115 mg, 0.852 mmol), and DMAP (8.3 mg, 56.8 μmol) in dry DMF (10 mL) was stirred for 10 min at 0 °C. Then the above crude amine (336 mg, 0.568 mmol) dissolved in dry DMF (5 mL) and DIPEA (148 μL, 0.852 mmol) were added to the above solution. The mixture was stirred at r.t. overnight. Upon completion of the reaction, the mixture was added brine (20 mL) and extracted with EtOAc (15 mL × 3). The organic extractions were combined, dried with anhydrous Na_2SO_4, and concentrated under vacuum. After the remaining DMF was removed by azeotropic distillation with toluene, the residue was purified by silica gel chromatography eluted with CH_2Cl_2/Acetone/MeOH (35/1/1) to afford **16A** as white foam (256 mg, 43% for 2 steps); R_f = 0.6, CH_2Cl_2/MeOH/Acetone = 10/1/1; ^{1}H NMR (400 MHz, $CDCl_3$) δ 11.55 (s, 1H), 8.61 (br, 1H), 8.41 (t, J = 5.6 Hz, 1H), 8.33 (d, J = 8.4 Hz, 1H), 7.86 (d, J = 8.4 Hz, 1H), 7.78 (d, J = 7.6 Hz, 1H), 7.70 (d, J = 8.0 Hz, 1H), 7.66–7.56 (m, 2H), 7.52 (d, J = 7.6 Hz, 1H), 7.47–7.14 (m, 10H), 6.89 (d, J = 7.6 Hz, 1H), 6.86–6.76 (m, 2H), 4.87 (br, 1H), 4.76 (d, J = 6.0 Hz, 1H), 4.61 (d, J = 11.2 Hz, 1H), 4.52–4.18 (m, 7H), 4.17–3.96 (m, 4H), 3.91–3.77 (m, 1H), 3.72–3.60 (m, 2H), 3.51 (dd, J = 11.2, 2.8 Hz, 1H), 3.48–3.37 (m, 1H), 2.97–2.81 (m, 1H), 2.80–2.60 (m, 1H), 2.54–2.04 (m, 8H), 2.01–1.70 (m, 3H), 1.62–1.46 (m, 1H), 1.43–1.08 (m, 13H), 0.77 (d, J = 6.0, 3H), 0.72 (d, J = 6.8 Hz, 3H); ^{13}C NMR (101 MHz, $CDCl_3$) δ 171.7, 171.4, 170.4, 170.2, 169.3, 169.2, 156.9, 156.0, 150.5, 141.7, 138.8, 133.8, 132.8, 132.2, 132.1, 131.9, 131.1, 130.6, 128.8, 127.9, 127.4, 126.9, 126.3, 125.8, 125.8, 125.5, 123.5, 123.5, 122.9, 122.8, 121.8, 121.1, 120.4, 112.1, 78.7, 77.2, 69.6, 67.1, 60.2, 58.8, 58.5, 56.1, 54.4, 53.4, 47.9, 47.1, 40.0, 39.8, 39.5, 39.4, 36.0, 31.6, 29.6, 29.2, 29.0, 28.8, 28.40, 28.35, 27.5, 25.2, 22.4, 18.9, 18.8, 16.0; HRMS: m/z $[M+H]^+$ Calcd. for $C_{66}H_{78}N_9O_{11}S$, 1204.5542 Found: 1204.5562.

tert-butyl ((S)-6-((2-((2-(2-(((2S,4S)-4-hydroxy-1-((S)-3-methyl-2-(1-oxoisoindolin-2-yl)butanoyl)pyrrolidine-2-carboxamido)methyl)-5-(4-methylthiazol-5-yl)phenoxy)ethyl)carbamoyl)phenyl)amino)-5-((S)-1-(2-(naphthalen-1-yl)acetyl)pyrrolidine-2-carboxamido)-6-oxohexyl)carbamate

16B.—The reaction was performed in the same way as **16A** starting with **15B** (180 mg, 0.292 mmol), 10% Pd/C (90.0 mg), **13A** (238 mg, 0.379 mmol), EDCI (84.0 mg, 0.437 mmol), HOAT (59.0 mg, 0.473 mmol), DMAP (4.30 mg, 35.0 μmol), and DIPEA (76.0 μL, 0.437 mmol) to give **16B** as white foam (150 mg, 43% for 2 steps); R_f = 0.6, CH_2Cl_2/MeOH/Acetone = 10/1/1; ^{1}H NMR (400 MHz, $CDCl_3$) δ 11.43 (s, 1H), 8.76 (s, 1H), 8.46 – 8.25 (m, 2H), 7.90 (dd, J = 35.2, 7.3 Hz, 2H), 7.78 (d, J = 7.2 Hz, 2H), 7.69 (d, J = 19.9 Hz, 2H), 7.58 – 7.28 (m, 10H), 6.99 (d, J = 7.1 Hz, 1H), 6.91 (s, 1H), 6.79 (s, 1H), 4.93 – 4.70 (m, 2H), 4.62 – 3.94 (m, 13H), 3.86 (d, J = 11.3 Hz, 1H), 3.71 (s, 2H), 3.55 (s, 1H), 3.04

Author Manuscript Author Manuscript Author Manuscript Author Manuscript

– 2.71 (m, 2H), 2.54 (s, 4H), 2.21 (d, J = 13.8 Hz, 2H), 1.90 (d, J = 44.5 Hz, 4H), 1.61 (s, 1H), 1.37 (s, 9H), 1.25 (br, 5H), 0.81 (s, 6H); ^{13}C NMR (101 MHz, $CDCl_3$) δ 171.7, 171.5, 171.3, 170.4, 169.3, 169.1, 157.0, 156.0, 150.7,147.9, 138.9, 133.9, 132.6, 132.3, 132.2, 131.9, 131.4, 130.8, 130.7, 128.8, 128.1, 127.9, 127.0, 126.4, 125.83, 125.6, 125.5, 123.7, 123.6, 123.1, 122.6, 122.0, 121.5, 121.0, 112.1, 78.7, 77.2, 70.6, 67.1, 60.2, 60.1, 58.4, 58.3, 54.4, 48.0, 40.4, 40.0, 39.7, 39.5, 35.3, 31.5, 29.1, 28.8, 28.4, 27.3, 25.3, 22.4, 19.0, 18.6, 15.8; HRMS: m/z $[M+H]^+$ Calcd. for $C_{66}H_{78}N_9O_{11}S$, 1204.5542 Found: 1204.5580.

tert-Butyl ((S)-6-((2-((2-(2-(2-(((2S,4R)-4-hydroxy-1-((S)-3-methyl-2-(1-oxoisoindolin-2-yl)butanoyl)pyrrolidine-2-carboxamido)methyl)-5-(4-methylthiazol-5-yl)phenoxy)ethoxy)ethyl)carbamoyl)phenyl)amino)-5-((S)-1-(2-(naphthalen-1-yl)acetyl)pyrolidine-2-carboxamido)-6-oxohexyl)carbamate 16C.—The reaction was performed in the same way as **16A** starting with **15C** (208 mg, 0.314 mmol), 10% Pd/C (100 mg), **13A** (260 mg, 0.412 mmol), EDCI (90.0 mg, 0.469 mmol), HOAT (64.0 mg, 0.473 mmol), DMAP (4.61 mg, 37.8 μmol), and DIPEA (82.0 μL, 0.472 mmol) to give **16C** as white foam (156 mg, 40% for 2 steps); R_f = 0.6, CH_2Cl_2/MeOH/Acetone = 10/1/1; ^{1}H NMR (400 MHz, $CDCl_3$) δ 11.67 (s, 1H), 8.72 (s, 1H), 8.47 (d, J = 8.4 Hz, 1H), 7.94 (d, J = 8.4 Hz, 1H), 7.85 (d, J = 8.0 Hz, 1H), 7.77 (d, J = 8.0 Hz, 1H), 7.72 (d, J = 7.6 Hz, 1H), 7.69–7.61 (m, 2H), 7.55–7.31 (m, 10H), 7.23 (d, J = 8.0 Hz, 1H), 6.96–6.89 (m, 2H), 6.85 (s, 1H), 4.93 (br, 1H), 4.83 (d, J = 5.2 Hz, 1H), 4.75 (d, J = 11.2 Hz, 1H), 4.61 (d, J = 18.0 Hz, 1H), 4.56–4.41 (m, 4H), 4.38–4.28 (m, 2H), 4.27–4.03 (m, 5H), 3.93–3.84 (m, 1H), 3.82–3.60 (m, 5H), 3.52 (q, J = 8.8 Hz, 1H), 3.46–3.34 (m, 1H), 3.01–2.87 (m, 1H), 2.85–2.73 (m, 1H), 2.50 (s, 3H), 2.46–2.37 (m, 1H), 2.37–2.27 (m, 1H), 2.26–2.10 (m, 2H), 2.09–2.02 (m, 1H), 1.97–1.91 (m, 2H), 1.90–1.79 (m, 1H), 1.66–1.55 (m, 1H), 1.36 (s, 9H), 1.32–1.20 (m, 4H), 0.96 (d, J = 6.4 Hz, 3H), 0.84 (d, J = 6.4 Hz, 3H); ^{13}C NMR (101 MHz, $CDCl_3$) δ 171.6, 171.4, 170.7, 170.4, 170.1, 169.4, 169.0, 156.8, 156.0, 150.6, 147.9, 142.0, 138.9, 133.8, 132.3, 132.1, 132.0, 131.8, 131.8, 131.4, 130.7, 129.9, 128.8, 127.9, 127.9, 127.2, 127.1, 127.0, 126.3, 125.8, 125.5, 123.6, 122.9, 122.2, 121.2, 120.4, 113.2, 78.7, 77.2, 69.9, 69.4, 69.2, 68.0, 60.2, 58.8, 58.6, 56.2, 54.3, 48.0, 47.4, 39.9, 39.5, 39.5, 39.2, 36.7, 31.6, 29.0, 28.9, 28.4, 27.5, 25.3, 22.3, 19.0, 15.9; HRMS: m/z $[M+H]^+$ Calcd. for $C_{68}H_{82}N_9O_{12}S$, 1248.5804 Found: 1248.5822.

tert-Butyl ((S)-6-((2-((2-(2-(2-(2-(2-(((2S,4R)-4-hydroxy-1-((S)-3-methyl-2-(1-oxoisoindolin-2-yl)butanoyl)pyrolidine-2-carboxamido)methyl)-5-(4-methylthiazol-5-yl)phenoxy)ethoxy)ethyl)carbamoyl)phenyl)amino)-5-((S)-1-(2-(naphthalen-1-yl)acetyl)pyrolidine-2-carboxamido)-6-oxohexyl)carbamate 16D.—The reaction was performed in the same way as **16A** starting with **15D** (238 mg, 0.318 mmol), Pd/C (115 mg), compound **13A** (260 mg, 0.412 mmol), EDCI (92.0 mg, 0.480 mmol), HOAT (64.4 mg, 0.477 mmol), DMAP (4.60 mg, 37.6 μmol), and DIPEA (83.0 μL, 0.477 mmol) to give **16C** as white foam (237 mg, 56% for 2 steps); R_f = 0.6, CH_2Cl_2/MeOH/Acetone = 10/1/1; ^{1}H NMR (400 MHz, $CDCl_3$) δ 11.60 (s, 1H), 8.62 (br, 1H), 8.41 (d, J = 8.0 Hz, 1H), 7.93–7.81 (m, 1H), 7.77 (d, J = 7.6 Hz, 1H), 7.68 (d, J = 8.0 Hz, 1H), 7.63 (d, J = 7.6 Hz, 2H), 7.54–7.15 (m, 12H), 6.96–6.82 (m, 2H), 6.78 (s, 1H), 4.97 (br, 1H), 4.81–4.57 (m, 3H), 4.56–4.35 (m, 3H), 4.35–4.21 (m, 3H), 4.16–3.89 (m, 5H), 3.84–3.66 (m, 2H), 3.66–3.31 (m, 14H), 2.94–

Author Manuscript Author Manuscript Author Manuscript Author Manuscript

2.74 (m, 1H), 2.70–2.60 (m, 1H), 2.42 (s, 3H), 2.37–2.21 (m, 2H), 2.17–1.68 (m, 6H), 1.60–1.46 (m, 1H), 1.27 (s, 9H), 1.23–1.08 (m, 4H), 0.91 (d, J = 6.4 Hz, 3H), 0.75 (d, J = 6.4 Hz, 3H); ^{13}C NMR (101 MHz, $CDCl_3$) δ 171.7, 171.1, 170.9, 170.3, 169.6, 168.9, 168.7, 156.5, 155.9, 150.2, 141.9, 138.8, 133.6, 132.0, 131.9, 131.5, 131.4, 130.6, 129.4, 128.6, 127.7, 127.7, 127.0, 126.8, 126.8, 126.2, 125.6, 125.4 123.5, 122.7, 122.6, 121.9, 121.0, 120.6, 112.5, 78.4, 77.2, 70.5, 70.1, 70.0, 69.69, 69.66, 69.4, 69.2, 67.7, 60.1, 58.7, 58.3, 55.9, 54.2, 47.8, 47.2, 39.7, 39.5, 39.3, 38.9, 37.1, 31.4, 28.9, 28.8, 28.2, 27.4, 25.1, 22.2, 18.9, 18.8, 16.0; HRMS: m/z $[M+H]^+$ Calcd. for $C_{72}H_{90}N_9O_{14}S$, 1336.6328 Found: 1336.6317.

(2S,4R)-N-(2-(2-(2-((S)-6-amino-2-((S)-1-(2-(naphthalen-1-yl)acetyl)pyrrolidine-2-carboxamido)hexanamido)benzamido)ethoxy)-4-(4-methylthiazol-5-yl)benzyl)-4-hydroxy-1-((S)-3-methyl-2-(1-oxoisoindolin-2-yl)butanoyl)pyrrolidine-2-carbox amide 1.—To a solution of **16A** (140 mg, 0.116 mmol) in CH_2Cl_2 (10 mL) was added 4M HCl in dioxane (2.6 mL) at 0 °C. The mixture was stirred at r.t. for 20 min followed by solvent removal under vacuum. The residue was purified by silica gel chromatography eluted with CH_2Cl_2/MeOH (from 20/1 to 10/1 to 5/1) to give **1** as white foam (101 mg, 78%); R_f = 0.3, CH_2Cl_2/MeOH = 8/1; ^{1}H NMR (400 MHz, CD_3OD) δ 8.85 (s, 1H), 8.35 (d, J = 8.0 Hz, 1H), 7.90 (t, J = 6.8 Hz, 2H), 7.82 (d, J = 8.0 Hz, 1H), 7.75 (d, J = 7.6 Hz, 1H), 7.65 (dd, J = 7.6, 1.2 Hz, 1H), 7.61–7.33 (m, 9H), 7.12–7.00 (m, 3H), 4.79 (d, J = 11.2 Hz, 1H), 4.59–4.53 (m, 1H), 4.52–4.42 (m, 6H), 4.39–4.34 (m, 1H), 4.30 (t, J = 5.2 Hz, 2H), 4.19 (q, J = 16.8 Hz, 2H), 3.97 (d, J = 11.2 Hz, 1H), 3.89–3.80 (m, 4H), 3.75–3.67 (m, 1H), 2.64–2.55 (m, 1H), 2.48 (s, 3H), 2.43–2.27 (m, 4H), 2.25–2.10 (m, 2H), 2.10–1.93 (m, 3H), 1.76–1.63 (m, 1H), 1.51–1.35 (m, 4H), 0.98 (d, J = 6.8 Hz, 3H), 0.78 (d, J = 6.4 Hz, 3H); ^{13}C NMR (101 MHz, CD_3OD) δ 175.6, 173.8, 172.7, 172.5, 170.9, 170.7, 158.2, 153.0, 149.2, 143.7, 139.5, 135.2, 133.6, 133.4, 133.3, 133.2, 133.1, 132.7, 132.4, 130.8, 129.8, 129.2, 129.1, 129.0, 128.6, 127.9, 127.5, 127.0, 126.6, 125.2, 124.7, 124.4, 124.4, 122.9, 122.8, 122.3, 113.3, 70.8, 67.9, 61.9, 60.7, 60.0, 57.2, 55.0, 40.6, 40.0, 39.0, 31.9, 30.8, 30.2, 27.1, 26.1, 23.4, 19.6, 19.0, 16.0; HRMS: m/z $[M+H]^+$ Calcd. for $C_{61}H_{70}N_9O_9S$, 1104.5017 Found: 1104.5010.

(2S,4R)-N-(2-(2-(2-(2-((S)-6-amino-2-((S)-1-(2-(naphthalen-1-yl)acetyl)pyrrolidine-2-carboxamido)hexanamido)benzamido)ethoxy)ethoxy)-4-(4-methyl-thiazol-5-yl)benzyl)-4-hydroxy-1-((S)-3-methyl-2-(1-oxoisoindolin-2-yl)butanoyl)pyrrolidine-2-carboxamide 2.—The reaction was performed in the same way as **1** starting with **16C** (75 mg, 60.1 μmol) and 4M HCl in dioxane (1.3 mL) to give **2** as white foam (61.4 mg, 89%); R_f = 0.3, CH_2Cl_2/MeOH = 8/1; ^{1}H NMR (400 MHz, CD_3OD) δ 8.86 (s, 1H), 8.39 (d, J = 8.0 Hz, 1H), 7.89 (t, J = 7.6 Hz, 2H), 7.81 (d, J = 7.6 Hz, 1H), 7.74 (d, J = 7.2 Hz, 1H), 7.65 (d, J = 7.6 Hz, 1H), 7.55–7.40 (m, 9H), 7.08 (t, J = 7.2 Hz, 1H), 7.03–6.98 (m, 2H), 4.81 (s, 1H), 4.65–4.33 (m, 8H), 4.30–4.06 (m, 4H), 4.05–3.87 (m, 4H), 3.81–3.61 (m, 4H), 3.66–3.50 (m, 2H), 2.70–2.56 (m, 1H), 2.49–2.33 (m, 7H), 2.28–2.10 (m, 2H), 2.08–1.93 (m, 3H), 1.79–1.64 (m, 1H), 1.51–1.30 (m, 4H), 1.01 (d, J = 6.0 Hz, 3H), 0.77 (d, J = 6.0 Hz, 3H); ^{13}C NMR (101 MHz, CD_3OD) δ 175.6, 174.0, 172.6, 172.5, 170.8, 170.6, 170.5, 157.9, 152.9, 149.0, 143.7, 139.5, 135.1, 133.5, 133.2, 133.0, 132.9, 132.7, 132.4, 129.9, 129.7, 129.1, 129.0, 128.6, 128.2, 127.4, 126.9,

Author Manuscript Author Manuscript Author Manuscript Author Manuscript

126.6, 125.2, 124.7, 124.4, 124.3, 122.8, 122.8, 122.2, 113.6, 70.8, 70.6, 69.5, 61.9, 60.7, 60.0, 57.1, 55.1, 54.9, 40.6, 40.5, 40.0, 39.3, 39.2, 31.8, 30.7, 30.1, 27.1, 26.1, 23.4, 19.7, 19.0, 16.0; HRMS: m/z $[M+H]^+$ Calcd. for $C_{63}H_{74}N_9O_{10}S$, 1148.5279 Found: 1148.5289.

(2S,4R)-N-(2-((1-(2-((S)-6-amino-2-((S)-1-(2-(naphthalen-1-yl)acetyl)pyrrolidine-2-carboxamido)hexanamido)phenyl)-1-oxo-5,8,11-trioxa-2-azatridecan-13-yl)oxy)-4-(4-methylthiazol-5-yl)benzyl)-4-hydroxy-1-((S)-3-methyl-2-(1-oxoisoindolin-2-yl)butanoyl)pyrrolidine-2-carboxamide 3.— The reaction was performed in the same way as **1** starting with **16D** (180 mg, 0.135 mmol), 4M HCl in dioxane (3 mL) to give **3** as white foam (120 mg, 72%); R_f = 0.3, CH_2Cl_2/MeOH = 8/1; ^{1}H NMR (400 MHz, CD_3OD) δ 8.87 (s, 1H), 8.41 (d, J = 8.4 Hz, 1H), 7.89 (t, J = 8.0 Hz, 2H), 7.81 (d, J = 8.0 Hz, 1H), 7.75 (d, J = 7.6 Hz, 1H), 7.70 (d, J = 7.6 Hz, 1H), 7.60–7.36 (m, 9H), 7.11 (t, J = 7.4 Hz, 1H), 7.05–6.96 (m, 2H), 4.82 (s, 1H), 4.62–4.56 (m, 3H), 4.52–4.34 (m, 5H), 4.27–4.07 (m, 4H), 3.98 (d, J = 11.2 Hz, 1H), 3.91–3.77 (m, 4H), 3.77–3.45 (m, 13H), 2.69–2.54 (m, 1H), 2.47 (s, 3H), 2.44–2.33 (m, 4H), 2.29–2.16 (m, 2H), 2.11–1.92 (m, 3H), 1.78–1.63 (m, 1H), 1.48–1.35 (m, 4H), 1.03 (d, J = 6.4 Hz, 3H), 0.79 (d, J = 6.8 Hz, 3H); ^{13}C NMR (101 MHz, CD_3OD) δ 175.6, 174.1, 172.6, 172.5, 170.8, 170.5, 170.4, 157.9, 152.9, 149.1, 143.7, 139.6, 135.1, 133.5, 133.4, 133.2, 133.1, 132.9, 132.7, 132.4, 129.9, 129.7, 129.1, 129.0, 128.6, 128.2, 127.4, 126.9, 126.6, 125.3, 124.6, 124.4, 124.4, 122.84, 122.79, 122.2, 113.7, 71.7, 71.5, 71.3, 70.8, 70.7, 70.4, 69.3, 61.9, 60.7, 60.0, 57.1, 55.0, 40.7, 40.5, 40.0, 39.4, 39.2, 31.8, 30.8, 30.1, 27.1, 26.1, 23.4, 19.7, 19.1, 16.1; HRMS: m/z $[M+H]^+$ Calcd. for $C_{67}H_{82}N_9O_{12}S$, 1236.5804 Found: 1236.5813.

(2S,4S)-N-(2-(2-(2-((S)-6-amino-2-((S)-1-(2-(naphthalen-1-yl)acetyl)pyrrolidine-2-carboxamido)hexanamido)benzamido)ethoxy)-4-(4-methylthiazol-5-yl)benzyl)-4-hydroxy-1-((S)-3-methyl-2-(1-oxoisoindolin-2-yl)butanoyl)-pyrrolidine-2-carboxamide 4.—The reaction was performed in the same way as **1** starting with **16B** (58.0 mg, 48.2 μmol), 4M HCl in dioxane (1 mL) to give **4** as white foam (40 mg, 75%); R_f = 0.3, CH_2Cl_2/MeOH = 8/1; ^{1}H NMR (400 MHz, CD_3OD) δ 8.85 (s, 1H), 8.18 (d, J = 8.1 Hz, 1H), 7.96 – 7.85 (m, 2H), 7.81 (d, J = 8.5 Hz, 1H), 7.77 (d, J = 7.6 Hz, 1H), 7.63 – 7.36 (m, 9H), 7.32 (t, J = 8.5 Hz, 1H), 7.09 – 6.91 (m, 3H), 4.79 (d, J = 11.0 Hz, 1H), 4.64 – 4.52 (m, 2H), 4.50 – 4.33 (m, 4H), 4.32 – 4.10 (m, 6H), 3.97 (dd, J = 11.4, 5.7 Hz, 1H), 3.92 – 3.77 (m, 3H), 3.76 – 3.66 (m, 2H), 2.69 – 2.58 (m, 1H), 2.47 (s, 3H), 2.44 – 2.29 (m, 4H), 2.27 – 2.20 (m, 1H), 2.13 (s, 1H), 2.05 – 1.93 (m, 2H), 1.90 – 1.83 (m, 1H), 1.75 – 1.65 (m, 1H), 1.47 – 1.34 (m, 4H), 0.94 – 0.89 (m, 3H), 0.79 (d, J = 6.6 Hz, 3H); ^{13}C NMR (101 MHz, CD_3OD) δ 175.5, 174.2, 172.7, 172.5, 170.9, 158.3, 153.0, 149.2, 143.7, 139.2, 135.2, 133.6, 133.4, 132.9, 132.8, 132.3, 131.0, 129.7, 129.3, 129.1, 129.0, 128.7, 127.7, 127.4, 126.9, 126.6, 125.3, 124.8, 124.5, 124.3, 124.0, 122.7, 122.6, 113.3, 71.1, 67.9, 61.9, 60.9, 59.8, 57.0, 55.0, 53.5, 50.8, 40.6, 40.5, 40.3, 40.0, 38.0, 31.8, 31.0, 30.0, 27.2, 26.1, 23.5, 19.5, 19.2, 16.0; HRMS: m/z $[M+H]^+$ Calcd. for $C_{61}H_{70}N_9O_9S$, 1104.5017 Found: 1104.4976.

Biology.

General Information—Purification of NTMT1 and its activity measurement were performed according to the published protocols.[19] A complete medium consists of McCoy's

Author Manuscript Author Manuscript Author Manuscript Author Manuscript

5A supplemented with 10% FBS (FB-02, Omega Scientific), 100 U/mL penicillin, and 100 μg/mL streptomycin. Cell lines HCT116 and HT29 were purchased from ATCC and *ntmt1* KO HCT116 was a gift from Prof. Christine Tooley (Buffalo University). They were cultured in a complete medium with 5% CO_2 at 37 °C. All drug treatments were performed by dissolving a stock solution of compound (30 mM in DMSO) into complete medium and then adding the mixture into plate wells. Primary antibodies used in Western blots were rabbit anti-actin (A2066, Sigma-Aldrich), rabbit anti-NTMT1 (ab102664, Abcam), rabbit anti-NTMT2 (NBP1–70635, Novus Biologicals or PA5–69586, ThermoFisher), and rabbit anti-CALR (10292–1-AP, Proteintech). All cell images were captured using Axio Vert.A1 inverted microscope (Zeiss) controlled by ZEN microscope software (Zeiss). Flow cytometry was performed at KUMC flow cytometry core facility using a FACSAria™ III flow cytometer (BD Biosciences). Cell cycles were analyzed using FlowJo. GraphPad Prism 9 was used to determine IC_{50} and DC_{50} as well as to perform unpaired t-tests. All biochemical and cellular experiments were done in triplicates.

Inhibition study of compounds 1–4 with purified NTMT1.—Inhibitory activities of **1**-**4** were monitored by HPLC at λ_{260} following the release of SAH. Adenosine was added as an internal standard. Briefly, in a final volume of 400 μL, 0.2 μM NTMT1, 6 μM SAM and the compound at various concentrations were incubated at 37 °C for 10 min in a buffer consisting of 50 mM KCl in 25 mM Tris (pH 7.5). Reaction was initiated by the addition of 2 μM RCC1 peptide [SPKRIAKRRS($CONH_2$)]. Aliquots of 50 μL were withdrawn at selected times and the reactions were quenched with 50 μL of 0.4% TFA solution containing 4.0 μM adenosine. The reaction mixtures were centrifuged at 18,000 *g* for 5 min. Fifty μL supernatants were injected into an XBridge Shield RP 18 column (3.5 μm, 130 Å, 4.6 × 150 mm, Waters) eluted at 1 mL/min with an isocratic gradient of 1% methanol in water supplemented with 0.01% TFA. Concentrations of released SAH were determined by A_{260} ratios of the peak areas corresponding to SAH and adenosine.

Cell culturing for Western blots.—A total of 8×10^4 cells were seeded per well in 6-well plates and cultured for 24 h. On the following day, cells were treated with either compounds **1**-**4** at various concentrations or DMSO for different times. Then, cells were washed with 1× PBS, harvested, and lysed at 4 °C for 1 h in a lysis buffer consisting of 150 mM NaCl, 50 mM Tris (pH 8.0), 0.5% NP-40, 0.5% Triton X-100, and protease inhibitor (A32955, ThermoFisher). Cell debris were removed by centrifugation at 17,000 *g* for 20 min at 4 °C. The resulting supernatant was collected and subjected to total protein quantification using a bicinchoninic acid (BCA) assay.

For pre-treatment experiments, cells were cultured for 22 h and then treated with 1 μM MG132 or 1 μM MLN4924 for additional 2 h. Degrader **1** (50 μM) or DMSO was then added to the medium and cells were cultured for another 24 h.

For washout assays, treated cells were washed with 1× PBS once and then cultured in fresh complete growth medium for another 10 and 20 h, at which time they were removed and processed for Western blots.

Author Manuscript Author Manuscript Author Manuscript Author Manuscript

Western blots.—Five μL protein ladder (1610374, BioRad) and 20 μg protein sample were loaded onto 10 % SDS-PAGE gel and subjected to electrophoresis for 30 min at 90 V followed by 1.5 h at 120V. Subsequently, all proteins were transferred to 0.2 μm PVDF (10600021, Cytiva), washed with 1 × TBST (1 × TBS + 0.1% Tween 20), and blocked with 5% fat-free milk in 1× TBST for 1 h. Bands corresponding to POIs and β-actin were cut out and incubated overnight at 4 °C with their respective primary antibodies diluted in 1× TBS supplemented with 5% BSA and 0.03% (w/v) sodium azide. Bands were then washed with 1× TBST for 5 min and the process repeated three additional times. After that, bands were incubated with a secondary antibody goat anti-rabbit IgG (AP132P, Sigma) for 1 h at r.t. followed by washing with 1× TBST (4 times, 5 min each time). Finally, bands were detected using a chemiluminescent reagent (34580, ThermoFisher or WBULS0100, Millipore), visualized using Amersham ImageQuant 800 (Cytiva), and quantified using ImageJ.

For dose-dependent and washout assays, Western blots were performed for NTMT1 and β-actin. For selectivity assays, bands corresponding to NTMT1, NTMT2, and β-actin were cut out for Western blots. For CALR detection, 10 μg protein sample was loaded onto 8% SDS-PAGE gel.

NTMT1 degradation visualized by fluorescence.—Plasmid *p*EGFP-n1-NTMT1 was constructed by inserting NTMT1 gene[19] into the mammalian expression vector pEGFP-n1 between *Xho*I and *EcoR*I using forward and reverse primers of TCAGATCTCGAGATGACGAGCGAGGTGATAGAAG and ACTGCAGAATTCTCTCAGGGCAAAGCTATAGACATG, respectively. For transfection, HCT116 cells were seeded in a 24-well plate at a density of 1.5×10^5 per well. After 12 h, medium was removed, and cells were washed twice with 1× PBS followed by addition of 450 μL 20% FBS in Corning transfectagro™ reduced-serum medium (TRSM) into each well. To prepare the transfect reagent, solution A consisting of 1.5 μL Lipofectamine 3000 (ThermoFisher) and 25 μL TRSM was mixed with solution B consisting of 1 mL P3000 reagent, 0.5 μg pEGFP-n1 or pEGFP-n1-NTMT1, and 25 μL TRSM. The mixture was incubated at r.t. for 15 min. The transfect reagent prepared was then added into each well and incubated for 8 h, at which time the medium was replaced with fresh complete medium and cells were allowed to recover for 24 h. After that, the cells were treated with 100 μM degrader **1** or DMSO for another 24 h before images were captured.

Cell viability assay.—A total of 5×10^3 cells were seeded per well in 96-well plates and cultured for 24 h. Cells were then treated with degrader **1** or negative control/inhibitor **4** at various concentrations, or DMSO for 72 h. Ten μL solution consisting of 5 mM WST-8 and 0.2 mM 1-methoxyphenazinium salt in 150 mM NaCl was added to each well and incubated for 3 h in the CO_2 incubator. Absorbance at 490 nm was determined using a SpectraMax® Plus 384 microplate reader (Molecular Devices).

Cell proliferation assay.—HCT116 cells (*wt* or KO) were seeded at 1×10^3 cells per well in 96-well plates and cultured for 24 h. Cells were then treated with degrader **1** or negative control/inhibitor **4** at various concentrations, or DMSO for 72 h. After medium was removed, cells were washed once with 1× PBS carefully and then stored in the microplate

Author Manuscript Author Manuscript Author Manuscript Author Manuscript

at −78 °C overnight. Next day, cells were thawed at r.t. Two hundred μL CyQUANT® GR dye/cell-lysis buffer (C7026, ThermoFisher) prepared according to manufacturer's protocol was added to each well. The plate was kept from light and incubated at r.t. for 10 min. Fluorescence was determined at λ_{480} (excitation) and λ_{520} (emission) using Synergy H1 hybrid multi-mode plate reader (BioTek).

Tumor spheroid assay with ultra-low surface attachment plate.—HCT116 cells were seeded at 1×10^3 cells per well in a 96-well round bottom ultra-low surface attachment plate (7007, Corning). After 3 days of incubation without disturbance, the spheroid was treated with degrader **1** or negative control/inhibitor **4** at various concentrations, or DMSO (day 0). Every 3 days post treatment, 90% medium in each well was carefully replaced with fresh complete medium containing degrader **1** or negative control/inhibitor **4**. Images were captured every 3 days and the volume of each tumor spheroid were determined according to the published protocol.[71]

Tumor spheroid assay with PG-S.—A mixture consisting of HCT116 cells harvested from 2D culture, 2% 3D PGmatrix-spheroid (PG-S) solution (PepGel Inc), and PGworks (PepGel Inc) at a ratio of 73:25:2 (v/v) was plated into a 48-well plate at 250 μL per well. The mixture was cultured for 30 min to trigger gel formation. The final hydrogel concentration was 0.5% (w/v) and contained 1×10^4 cells per well. Then 800 μL complete medium was placed in each well to feed cells. HCT116 were allowed to grow within PG-S for 3 days followed by treatment with degrader **1** or negative control/inhibitor **4** at various concentrations, or DMSO for additional 3 days. Cells were then harvested for determination of cell number and viability. To isolate cells from 3D culture, the hydrogel was thoroughly disrupted by pipetting and mixed well with the medium on top. The mixture was then transferred to a conical tube. Each well was rinsed with 1 mL Dulbecco's phosphate buffered saline (DPBS), which was combined into the conical tube. Additional DPBS was used to dilute the cell-gel mixture from each well to a total volume of 5 mL. The diluted mixture was centrifuged at 800 *g* for 5 min, and HCT116 spheroid pellets were collected. To obtain single HCT116 cell, spheroid pellets were treated with 0.25% trypsin-EDTA at 0.75 mL per tube for 30 min at 37 °C. Trypsinization was terminated by adding 0.75 mL complete medium to each tube. Cell suspension was then centrifuged at 200 *g* for 5 min to obtain single cells. After images of cell spheroids were captured, cells were stained with acridine orange/propidium iodide (AO/PI) and then analyzed by automatic cell counting using Cellometer Auto 2000 (Nexcelom Bioscience LLC). Cell viability percentage was calculated as the number of live cells in the total number of live and dead cells.

Flow cytometry assay.—HCT116 cells were seeded at 8×10^4 per well in 6-well plates. After 24 h, the cells were treated with degrader **1** at various concentrations or DMSO for 72 h. Subsequently, cells were washed with 1× PBS and then harvested after trypsinization. For each sample, 4×10^5 cells were resuspended in a 2.0 mL tube (pre-coated with 2% BSA in 1× PBS overnight), washed twice with 1 mL 1× PBS (supernatant was removed after centrifugation at 500 *g* and 4 °C for 10 min) and resuspended in 0.1 mL 1× PBS. Vortexed gently, slowly adding the cell suspension dropwise to 1 mL 70% ethanol pre-cooled to −20 °C. The ethanol suspension was stored at −20 °C for 12 h. Supernatants was removed after

Author Manuscript Author Manuscript Author Manuscript Author Manuscript

centrifugation at 1,000 *g* for 10 min at 4 °C. Cells were washed twice with 1 mL ice cold 1× PBS (supernatant was removed after centrifugation at 1,000 *g* for 10 min at 4 °C). The pellet was resuspended in 500 μL staining solution (consisting of 0.5 μL Triton X-100, 0.1 mg DNase-free RNase A, and 10 μg PI in 1× PBS) and incubated at r.t. for 30 min. The tube protected from light was then kept in ice until analysis. Flow cytometry was performed on a FACSAria™ III flow cytometer (BD Biosciences). Ten thousand cells were collected for each sample.

Mass spectrometry assay.—Samples were prepared as follows: HCT116 cells treated with either degrader **1** or negative control/inhibitor **4** at 25 μM for 24 h were washed with 1× PBS, harvested and lysed by sonication for 20s (5s on, 5s off, 20% amplitude) in 1× TBS supplemented with protease inhibitor (A32955, ThermoFisher). Total protein concentrations were determined by BCA assays. One hundred μg proteins were loaded onto an S-Trap™ column (ProtiFi, Farmingdale, NY) following manufacturer's protocol and digested with trypsin in a ratio of 10:1 (V5111, Promega). Peptide elution was dried by speed-vac and resuspended in a solution consisting of 0.1% formic acid in acetonitrile/water mixture (1/1, v/v). Prepared samples were injected into a Waters LC/MS system. LC was performed with an analytical column (ACQUITY UPLC M-Class HSS T3 Column, 1.8 μm, 100Å, 300 μm × 150 mm, Waters) eluted at 3.0 μL/min with a gradient of acetonitrile (containing 0.1% formic acid) from 1% to 60% in 70 min and then from 60% to 70% in 10 min in water (containing 0.1% formic acid). Elution from UPLC was nanosprayed with 3.0 kV capillary voltages and the mass spectrometer was operated under an MSE mode for data-independent acquisition. Raw data were processed and analyzed using Progenesis QI for Proteomics. Data were first automatically analyzed by specifying threshold intensities at 250 counts for low energy and 150 counts for elevated energy. Subsequently, peptides that have ≥ 6 amino acids were selected manually. Criteria for protein identification search were set as follows: two possible missed cleavage sites for trypsin digestion, one fixed modification of cysteine carbamidomethylation, one variable modification of methionine oxidation, UniProt proteome (ID: UP000005640) as the search database, and quantification by non-conflicting peptides. Ion matching requirements were set as follows: peptides/protein ≥ 1, fragments/peptide ≥ 1, and fragments/protein ≥ 3. A list of proteins identified is shown in the Excel file in Supplementary Data.

Supplementary Material

Refer to Web version on PubMed Central for supplementary material.

ACKNOWLEDGMENT

This work was supported in part by NIH R01GM117259, COBRE grant P30GM110761 pilot project, and Johnson Cancer Center Innovative Research Award to P.L. We acknowledge National Science Foundation for the purchase of 400 MHz NMR spectrometer under grant 1826982. We also acknowledge the Flow Cytometry Core Laboratory at KUMC, which is sponsored, in part, by the NIH/NIGMS COBRE grant P30GM103326 and the NIH/NCI Cancer Center grant P30CA168524. We thank Prof. Christine Tooley (Buffalo University) for providing us *ntmt1* KO HCT116 cells. We also thank Jordan Gipper for helping to prepare compound **11**.

Author Manuscript Author Manuscript Author Manuscript Author Manuscript

DATA AVAILABILITY

Data will be made available upon request.

REFERENCES

1. Clarke SG, The ribosome: A hot spot for the identification of new types of protein methyltransferases, J. Biol. Chem, 293 (2018) 10438–10446. [PubMed: 29743234]
2. Diaz K, Meng Y, Huang R, Past, present, and perspectives of protein N-terminal methylation, Curr. Opin. Chem. Biol 63 (2021) 115–122. [PubMed: 33839647]
3. Stock A, Clarke S, Clarke C, Stock J, N-Terminal methylation of proteins−Structure, function and specificity, FEBS Lett. 220 (1987) 8–14. [PubMed: 3301412]
4. Huang R, Chemical biology of protein N-terminal methyltransferases, ChemBioChem 20 (2019) 976–984. [PubMed: 30479015]
5. Brosius J, Chen R, The primary structure of protein L16 located at the peptidyltransferase center of *Escherichia coli* ribosomes, FEBS Lett. 68 (1976) 105–109. [PubMed: 786730]
6. Chang CN, Schwartz M, Chang FN, Identification and characterization of a new methylated amino acid in ribosomal protein L33 of *Escherichia coli*., Biochem. Biophys. Res. Commun 73 (1976) 233–239. [PubMed: 793594]
7. Wittmann-Liebold B, Pannenbecker R, Primary structure of protein L33 from the large subunit of the *Escherichia coli* ribosome, FEBS Lett. 68 (1976) 115–118. [PubMed: 786732]
8. Tooley CES, Petkowski JJ, Muratore-Schroeder TL, Balsbaugh JL, Shabanowitz J, Sabat M, Minor W, Hunt DF, Macara IG, NRMT is an alpha-N-methyltransferase that methylates RCC1 and retinoblastoma protein, Nature 466 (2010) 1125–1128. [PubMed: 20668449]
9. Webb KJ, Lipson RS, Al-Hadid Q, Whitelegge JP, Clarke SG, Identification of protein N-terminal methyltransferases in yeast and humans, Biochemistry 49 (2010) 5225–5235. [PubMed: 20481588]
10. Martinage A, Briand G, Vandorsselaer A, Turner CH, Sautiere P, Primary structure of histone H2b from gonads of the starfish *Asterias-Rubens*−Identification of an N-dimethylproline residue at the amino-terminal, Eur. J. Biochem 147 (1985) 351–359. [PubMed: 3882426]
11. Nomoto M, Kyogoku Y, Iwai K, N-Trimethylalanine, a novel blocked N-terminal residue of *Tetrahymena* histone H2B, J. Biochem 92 (1982) 1675–1678. [PubMed: 6818230]
12. Henry GD, Trayer IP, Brewer S, Levine BA, The widespread distribution of α-N-trimethylalanine as the N-terminal amino-acid of light-chains from vertebrate striated-muscle myosins, Eur. J. Biochem 148 (1985) 75–82. [PubMed: 3979397]
13. Trayer P, Trayer HR, Levine BA, Evidence that the N-terminal region of A1-light chain of myosin interacts directly with the C-terminal region of actin−A proton magnetic-resonance study, Eur. J. Biochem 164 (1987) 259–266. [PubMed: 3549306]
14. Bailey AO, Panchenko T, Sathyan KM, Petkowski JJ, Pai PJ, Bai DL, Russell DH, Macara IG, Shabanowitz J, Hunt DF, Black BE, Foltz DR, Posttranslational modification of CENP-A influences the conformation of centromeric chromatin, Proc. Natl. Acad. Sci. U.S.A 110 (2013) 11827–11832. [PubMed: 23818633]
15. Cai Q, Fu LJ, Wang Z, Gan NQ, Dai XX, Wang YS, alpha-N-Methylation of damaged DNA-binding protein 2 (DDB2) and its function in nucleotide excision repair, J. Biol. Chem 289 (2014) 16046–16056. [PubMed: 24753253]
16. Chen T, Muratore TL, Schaner-Tooley CE, Shabanowitz J, Hunt DF, Macara IG, N-terminal α-methylation of RCC1 is necessary for stable chromatin association and normal mitosis, Nat. Cell Biol 9 (2007) 596–U203. [PubMed: 17435751]
17. Dai XX, Otake K, You CJ, Cai Q, Wang Z, Masumoto H, Wang YS, Identification of novel α-N-methylation of CENP-B that regulates its binding to the centromeric DNA, J. Proteome Res 12 (2013) 4167–4175. [PubMed: 23978223]
18. Dai XX, Rulten SL, You C, Caldecott KW, Wang YS, Identification and functional characterizations of N-terminal α-N-methylation and phosphorylation of serine 461 in human poly(ADP-ribose) polymerase 3, J. Proteome Res 14 (2015) 2575–2582. [PubMed: 25886813]

Author Manuscript Author Manuscript Author Manuscript Author Manuscript

19. Jia M, Huang GC, Wu W, Shrestha R, Wu BB, Xiong YL, Li P, *In vivo* methylation of OLA1 revealed by activity-based target profiling of NTMT1, Chem. Sci 10 (2019) 8094–8099. [PubMed: 31857877]
20. Nevitt C, Tooley JG, Tooley CES, N-terminal acetylation and methylation differentially affect the function of MYL9, Biochem. J 475 (2018) 3201–3219. [PubMed: 30242065]
21. England R, Huang JH, Jennings MJ, Makde RD, Tan S, RCC1 uses a conformationally diverse loop region to interact with the nucleosome: A model for the RCC1-nucleosome complex, J. Mol. Biol 398 (2010) 518–529. [PubMed: 20347844]
22. Tooley JG, Tooley CES, New roles for old modifications: Emerging roles of N-terminal post-translational modifications in development and disease, Protein Sci. 23 (2014) 1641–1649. [PubMed: 25209108]
23. Shields M, Tooley JG, Petkowski JJ, Wilkey DW, Garbett NC, Merchant ML, Cheng A, Tooley CES, Select human cancer mutants of NRMT1 alter its catalytic activity and decrease N-terminal trimethylation, Protein Sci. 26 (2017) 1639–1652. [PubMed: 28556566]
24. Bonsignore A, Butler JS, Klinge CM, Schaner Tooley CE, Loss of the N-terminal methyltransferase NRMT1 increases sensitivity to DNA damage and promotes mammary oncogenesis, Oncotarget 6 (2015) 12248–12263. [PubMed: 25909287]
25. Bonsignore LA, Tooley JG, Van Hoose PM, Wang E, Cheng A, Cole MP, Tooley CES, NRMT1 knockout mice exhibit phenotypes associated with impaired DNA repair and premature aging, Mech. Ageing Dev 146 (2015) 42–52. [PubMed: 25843235]
26. Hong Y, Downey T, Eu KW, Koh PK, Cheah PY, A 'metastasis-prone' signature for early-stage mismatch-repair proficient sporadic colorectal cancer patients and its implications for possible therapeutics, Clin. Exp. Metastasis 27 (2010) 83–90. [PubMed: 20143136]
27. Kaiser S, Park YK, Franklin JL, Halberg RB, Yu M, Jessen WJ, Freudenberg J, Chen XD, Haigis K, Jegga AG, Kong S, Sakthivel B, Xu H, Reichling T, Azhar M, Boivin GP, Roberts RB, Bissahoyo AC, Gonzales F, Bloom GC, Eschrich S, Carter SL, Aronow JE, Kleimeyer J, Kleimeyer M, Ramaswamy V, Settle SH, Boone B, Levy S, Graff JM, Doetschman T, Groden J, Dove WF, Threadgill DW, Yeatman TJ, Coffey RJ, Aronow BJ, Transcriptional recapitulation and subversion of embryonic colon development by mouse colon tumor models and human colon cancer, Genome Biol. 8 (2007) R131. [PubMed: 17615082]
28. Sabates-Beliver J, Van der Flier LG, de Palo M, Cattaneo E, Maake C, Rehrauer H, Laczko E, Kurowski MA, Bujnicki JM, Menigatti M, Luz J, Ranalli TV, Gornes V, Pastorelli A, Faggiani R, Anti M, Jiricny J, Clevers H, Marra G, Transcriptome profile of human colorectal adenomas, Mol. Cancer Res 5 (2007) 1263–1275. [PubMed: 18171984]
29. Rawla P, Sunkara T, Barsouk A, Epidemiology of colorectal cancer: incidence, mortality, survival, and risk factors, Gastroenterology Rev. 14 (2019) 89–103.
30. Chen DX, Dong GP, Noinaj N, Huang R, Discovery of bisubstrate inhibitors for protein N-terminal methyltransferase 1, J. Med. Chem 62 (2019) 3773–3779. [PubMed: 30883119]
31. Zhang G, Huang R, Facile synthesis of SAM-peptide conjugates through alkyl linkers targeting protein N-terminal methyltransferase 1, RSC. Adv 6 (2016) 6768–6771. [PubMed: 27588169]
32. Zhang G, Richardson SL, Mao YF, Huang R, Design, synthesis, and kinetic analysis of potent protein N-terminal methyltransferase 1 inhibitors, Org. Biomol. Chem 13 (2015) 4149–4154. [PubMed: 25712161]
33. Chen DX, Dong GP, Deng YC, Noinaj N, Huang R, Structure-based discovery of cell-potent peptidomimetic inhibitors for protein N-terminal methyltransferase 1, ACS. Med. Chem. Lett 12 (2021) 485–493. [PubMed: 33738076]
34. Mackie BD, Chen DX, Dong GP, Dong C, Parker H, Tooley CES, Noinaj N, Min JR, Huang R, Selective peptidomimetic inhibitors of NTMT1/2: Rational design, synthesis, characterization, and crystallographic studies, J. Med. Chem 63 (2020) 9512–9522. [PubMed: 32689795]
35. Chen DX, Dong C, Dong GP, Srinivasan K, Min JR, Noinaj N, Huang R, Probing the plasticity in the active site of protein N-terminal methyltransferase 1 using bisubstrate analogues, J. Med. Chem 63 (2020) 8419–8431. [PubMed: 32605369]
36. Burslem GM, Crews CM, Proteolysis-targeting chimeras as therapeutics and tools for biological discovery, Cell 181 (2020) 102–114. [PubMed: 31955850]

Author Manuscript Author Manuscript Author Manuscript Author Manuscript

37. Bond J, Crews CM, Proteolysis targeting chimeras (PROTACs) come of age: Entering the third decade of targeted protein degradation, RSC. Chem. Biol 2 (2021) 725–742. [PubMed: 34212149]
38. Winter GE, Buckley DL, Paulk J, Roberts JM, Souza A, Dhe-Paganon S, Bradner JE, Phthalimide conjugation as a strategy for *in vivo* target protein degradation, Science 348 (2015) 1376–1381. [PubMed: 25999370]
39. Bondeson DP, Mares A, Smith IED, Ko E, Campos S, Miah AH, Mulholland KE, Routly N, Buckley DL, Gustafson JL, Zinn N, Grandi P, Shimamura S, Bergamini G, Faelth-Savitski M, Bantscheff M, Cox C, Gordon DA, Willard RR, Flanagan JJ, Casillas LN, Votta BJ, den Besten W, Famm K, Kruidenier L, Carter PS, Harling JD, Churcher I, Crews CM, Catalytic in vivo protein knockdown by small-molecule PROTACs, Nat. Chem. Biol 11 (2015) 611–617. [PubMed: 26075522]
40. Burslem GM, Smith BE, Lai AC, Jaime-Figueroa S, McQuaid DC, Bondeson DP, Toure M, Dong HQ, Qian YM, Wang J, Crew AP, Hines J, Crews CM, The advantages of targeted protein degradation over inhibition: An RTK case study, Cell Chem. Biol 25 (2018) 67–77. [PubMed: 29129716]
41. Gechijian LN, Buckley DL, Lawlor MA, Reyes JM, Paulk J, Ott CJ, Winter GE, Erb MA, Scott TG, Xu MS, Seo HS, Dhe-Paganon S, Kwiatkowski NP, Perry JA, Qi J, Gray NS, Bradner JE, Functional TRIM24 degrader via conjugation of ineffectual bromodomain and VHL ligands, Nat. Chem. Biol 14 (2018) 405–412. [PubMed: 29507391]
42. Kerres, Steurer S, Schlager S, Bader G, Berger H, Caligiuri M, Dank C, Engen JR, Ettmayer P, Fischerauer B, Flotzinger G, Gerlach D, Gerstberger T, Gmaschitz T, Greb P, Han BS, Heyes E, Iacob RE, Kessler D, Kolle H, Lamarre L, Lancia DR, Lucas S, Mayer M, Mayr K, Mischerikow N, Muck K, Peinsipp C, Petermann O, Reiser U, Rudolph D, Rumpel K, Salomon C, Scharn D, Schnitzer R, Schrenk A, Schweifer N, Thompson D, Traxler E, Varecka R, Voss T, Weiss-Puxbaum A, Winkler S, Zheng XZ, Zoephel A, Kraut N, McConnell D, Pearson M, Koegl M, Chemically induced degradation of the oncogenic transcription factor BCL6, Cell Rep. 20 (2017) 2860–2875. [PubMed: 28930682]
43. Raina K, Lu J, Qian YM, Altieri M, Gordon D, Rossi AMK, Wang J, Chen X, Dong HQ, Siu K, Winkler JD, Crew AP, Crews CM, Coleman KG, PROTAC-induced BET protein degradation as a therapy for castration-resistant prostate cancer, Proc. Natl. Acad. Sci. U.S.A 113 (2016) 7124–7129. [PubMed: 27274052]
44. Gadd MS, Testa A, Lucas X, Chan KH, Chen WZ, Lamont DJ, Zengerle M, Ciulli A, Structural basis of PROTAC cooperative recognition for selective protein degradation, Nat. Chem. Biol 13 (2017) 514–521. [PubMed: 28288108]
45. Bondeson DP, Smith BE, Burslem GM, Buhimschi AD, Hines J, Jaime-Figueroa S, Wang J, Hamman BD, Ishchenko A, Crews CM, Lessons in PROTAC design from selective degradation with a promiscuous warhead, Cell Chem. Biol 25 (2018) 78–87. [PubMed: 29129718]
46. Lai AC, Crews CM, Induced protein degradation: An emerging drug discovery paradigm, Nat. Rev. Drug Discov 16 (2017) 101–114. [PubMed: 27885283]
47. Buhimschi D, Armstrong HA, Toure M, Jaime-Figueroa S, Chen TL, Lehman AM, Woyach JA, Johnson AJ, Byrd JC, Crews CM, Targeting the C481S ibrutinib-resistance mutation in bruton's tyrosine kinase using PROTAC-mediated degradation, Biochemistry 57 (2018) 3564–3575. [PubMed: 29851337]
48. Mullard, Targeted protein degraders crowd into the clinic, Nat. Rev. Drug Discov 20 (2021) 247–250. [PubMed: 33737725]
49. Lu J, Qian YM, Altieri M, Dong HQ, Wang J, Raina K, Hines J, Winkler JD, Crew AP, Coleman K, Crews CM, Hijacking the E3 ubiquitin ligase cereblon to efficiently target BRD4, Chem. Biol 22 (2015) 755–763. [PubMed: 26051217]
50. Piya S, Mu H, Bhattacharya S, Lorenzi PL, Davis RE, McQueen T, Ruvolo V, Baran N, Wang Z, Qian Y, Crews CM, Konopleva M, Ishizawa J, You MJ, Kantarjian H, Andreeff M, Borthakur G, BETP degradation simultaneously targets acute myelogenous leukemia stem cells and the microenvironment, J. Clin. Investig 129 (2019) 1878–1894. [PubMed: 30829648]
51. Burslem GM, Song JY, Chen X, Hines J, Crews CM, Enhancing antiproliferative activity and selectivity of a FLT-3 inhibitor by proteolysis targeting chimera conversion, J. Am. Chem. Soc 140 (2018) 16428–16432. [PubMed: 30427680]

Author Manuscript Author Manuscript Author Manuscript Author Manuscript

52. Ward C, Kleinman JI, Brittain SM, Lee PS, Chung CYS, Kim K, Petri Y, Thomas JR, Tallarico JA, McKenna JM, Schirle M, Nomura DK, Covalent ligand screening uncovers a RNF4 E3 ligase recruiter for targeted protein degradation applications, ACS. Chem. Biol 14 (2019) 2430–2440. [PubMed: 31059647]
53. He YH, Zhang X, Chang JH, Kim HN, Zhang PY, Wang YY, Khan S, Liu XG, Zhang X, Lv DW, Song L, Li W, Thummuri D, Yuan YX, Wiegand JS, Ortiz YT, Budamagunta V, Elisseeff JH, Campisi J, Almeida M, Zheng GR, Zhou DH, Using proteolysis-targeting chimera technology to reduce navitoclax platelet toxicity and improve its senolytic activity, Nat. Commun 11 (2020) 1996. [PubMed: 32332723]
54. Bricelj A, Steinebach C, Kuchta R, Gütschow M, Sosič I, E3 ligase ligands in successful PROTACs: An overview of syntheses and linker attachment points, Front. Chem 9 (2021) 707317. [PubMed: 34291038]
55. Zhang L, Riley-Gillis B, Vijay P, Shen Y, Acquired resistance to BET-PROTACs (proteolysis-targeting chimeras) caused by genomic alterations in core components of E3 ligase complexes, Mol. Cancer Ther 18 (2019) 1302–1311. [PubMed: 31064868]
56. Cecchini, Pannilunghi S, Tardy S, Scapozza L, From conception to development: Investigating PROTACs features for improved cell permeability and successful protein degradation,Front. Chem 9 (2021) 672267. [PubMed: 33959589]
57. Klein VG, Townsend CE, Testa A, Zengerle M, Maniaci C, Hughes SJ, Chan KH, Ciulli A, Lokey RS, Understanding and improving the membrane permeability of VH032-based PROTACs, ACS. Med. Chem. Lett 11 (2020) 1732–1738. [PubMed: 32939229]
58. Steinebach, Voell SA, Vu LP, Bricelj A, Sosic I, Schnakenburg G, Gutschow M, A facile synthesis of ligands for the von Hippel-Lindau E3 ligase, Synthesis 52 (2020) 2521–2527.
59. Ma JJ, Chen L, Fan JB, Cao W, Zeng GY, Wang YJ, Li YJ, Zhou YJ, Deng X, Dual-targeting Rutaecarpine-NO donor hybrids as novel anti-hypertensive agents by promoting release of CGRP, Eur. J. Med. Chem 168 (2019) 146–153. [PubMed: 30818175]
60. Frost J, Galdeano C, Soares P, Gadd MS, Grzes KM, Ellis L, Epemolu O, Shimamura S, Bantscheff M, Grandi P, Read KD, Cantrell DA, Rocha S, Ciulli A, Potent and selective chemical probe of hypoxic signalling downstream of HIF-α hydroxylation via VHL Inhibition, Nat. Commun 7 (2016) 13312. [PubMed: 27811928]
61. Roth S, Fulcher LJ, Sapkota GP, Advances in targeted degradation of endogenous proteins, Cell. Mol. Life Sci 76 (2019) 2761–2777. [PubMed: 31030225]
62. Petkowski JJ, Bonsignore LA, Tooley JG, Wilkey DW, Merchant ML, Macara IG, Schaner Tooley CE, NRMT2 is an N-terminal monomethylase that primes for its homologue NRMT1, Biochem. J 456 (2013) 453–462. [PubMed: 24090352]
63. Dong, Dong GP, Li L, Zhu LC, Tempel W, Liu YL, Huang R, Min JR, An asparagine/glycine switch governs product specificity of human N-terminal methyltransferase NTMT2, Commun. Biol 1 (2018) 183. [PubMed: 30417120]
64. Wu RX, Yue Y, Zheng XD, Li HT, Molecular basis for histone N-terminal methylation by NRMT1, Gene Dev. 29 (2015) 2337–2342. [PubMed: 26543159]
65. Dong, Mao YF, Tempel W, Qin S, Li L, Loppnau P, Huang R, Min JR, Structural basis for substrate recognition by the human N-terminal methyltransferase 1, Gene Dev. 29 (2015) 2343–2348. [PubMed: 26543161]
66. Tominaga H, Ishiyama M, Ohseto F, Sasamoto K, Hamamoto T, Suzuki K, Watanabe M, A water-soluble tetrazolium salt useful for colorimetric cell viability assay, Anal. Commun 36 (1999) 47–50.
67. Jensen, Teng Y, Is it time to start transitioning from 2D to 3D cell culture? Front. Mol. Biosci 7 (2020) :33. [PubMed: 32211418]
68. Lee J, Cuddihy MJ, Kotov NA, Three-dimensional cell culture matrices: State of the art, Tissue Eng. Part B Rev 14 (2008) 61–86. [PubMed: 18454635]
69. Pampaloni, Reynaud EG, Stelzer EHK, The third dimension bridges the gap between cell culture and live tissue, Nat. Rev. Mol. Cell Bio 8 (2007) 839–845. [PubMed: 17684528]
70. Xu JW, Qi GY, Wang WQ, Sun XS, Advances in 3D peptide hydrogel models in cancer research,npj Sci. Food 5 (2021) 14. [PubMed: 34075054]

Author Manuscript Author Manuscript Author Manuscript Author Manuscript

71. Thippabhotla S, Zhong CC, He M, 3D cell culture stimulates the secretion of *in vivo* like extracellular vesicles, Sci. Rep 9 (2019) 13012. [PubMed: 31506601]

72. Fucikova J, Spisek R, Kroemer G, Galluzzi L, Calreticulin and cancer, Cell Res. 31 (2021) 5–16. [PubMed: 32733014]

73. Schcolnik-Cabrera A, Oldak B, Juarez M, Cruz-Rivera M, Flisser A, Mendlovic F, Calreticulin in phagocytosis and cancer: opposite roles in immune response outcomes, Apoptosis 24 (2019) 245–255. [PubMed: 30929105]

74. Fucikova J, Kepp O, Kasikova L, Petroni G, Yamazaki T, Liu P, Zhao LW, Spisek R, Kroemer G, Galluzzi L, Detection of immunogenic cell death and its relevance for cancer therapy, Cell Death Discov. 11 (2020) 1013.

75. Bezu L, Kepp O, Cerrato G, Pol J, Fucikova J, Spisek R, Zitvogel L, Kroemer G, Galluzzi L, Trial watch: Peptide-based vaccines in anticancer therapy, Oncoimmunology 7 (2018) e1511506. [PubMed: 30524907]

76. Kasikova L, Hensler M, Truxova I, Skapa P, Laco J, Belicova L, Praznovec I, Vosahlikova S, Halaska MJ, Brtnicky T, Rob L, Presl J, Kostun J, Cremer I, Ryska A, Kroemer G, Galluzzi L, Spisek R, Fucikova J, Calreticulin exposure correlates with robust adaptive antitumor immunity and favorable prognosis in ovarian carcinoma patients, J. Immunother. Cancer 7 (2019) 312. [PubMed: 31747968]

77. Han A, Li C, Zahed T, Wong M, Smith I, Hoedel K, Green D, Boiko AD, Calreticulin is a critical cell survival factor in malignant neoplasms. PLOS Biol. 17 (2019) e3000402. [PubMed: 31568485]

78. Peng RQ, Chen YB, Ding Y, Zhang R, Zhang X, Yu XJ, Zhou ZW, Zeng YX, Zhang XS, Expression of calreticulin is associated with infiltration of T-cells in stage IIIB colon cancer, World J. Gastroenterol 16 (2010) 2428–2434. [PubMed: 20480531]

79. Toquet C, Jarry A, Bou-Hanna C, Bach K, Denis MG, Mosnier JF, Laboisse CL, Altered calreticulin expression in human colon cancer: Maintenance of calreticulin expression is associated with mucinous differentiation, Oncol. Rep 17 (2007) 1101–1107. [PubMed: 17390051]

80. Colangelo T, Polcaro G, Ziccardi P, Muccillo L, Galgani M, Pucci B, Milone MR, Budillon A, Santopaolo M, Mazzoccoli G, Matarese G, Sabatino L, Colantuoni V, The miR-27a-Calreticulin axis affects drug-induced immunogenic cell death in human colorectal cancer cells. Cell Death Discov. 7 (2016) e2108.

81. Rijkers TS, Adams HPHM, Hemker HC, Tesser GI, A Convenient synthesis of amino-acid P-nitroanilides: Synthons in the synthesis of protease substrates, Tetrahedron 51 (1995) 11235–11250.

Author Manuscript Author Manuscript Author Manuscript Author Manuscript

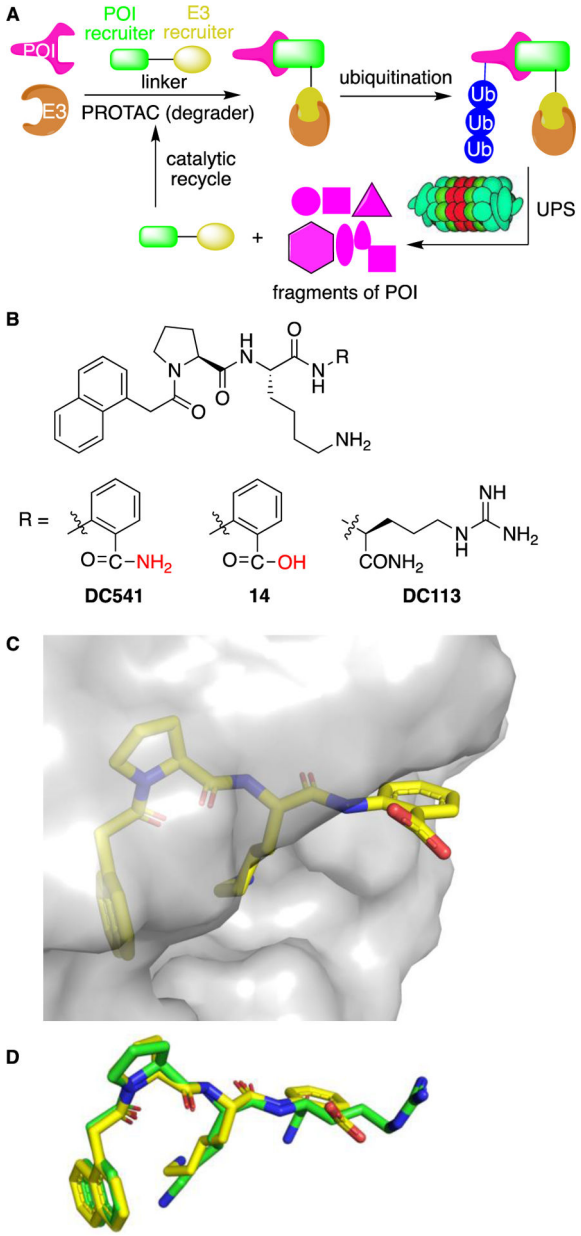

Figure 1.

Design of PROTAC molecules (degraders) targeting NTMT1. (A) Principles of PROTAC action. (B) Chemical structures of NTMT1 inhibitors. (C) Docking result of compound **14** bound with NTMT1 using an online SwissDock server (http://www.swissdock.ch/docking). Model was prepared by PyMol. Protein surface and compound **14** are shown in grey and yellow, respectively. (D) Overlay of compound **14** (yellow) and DC113 (green, PDB 7K3D) bound with NTMT1.

Author Manuscript Author Manuscript Author Manuscript Author Manuscript

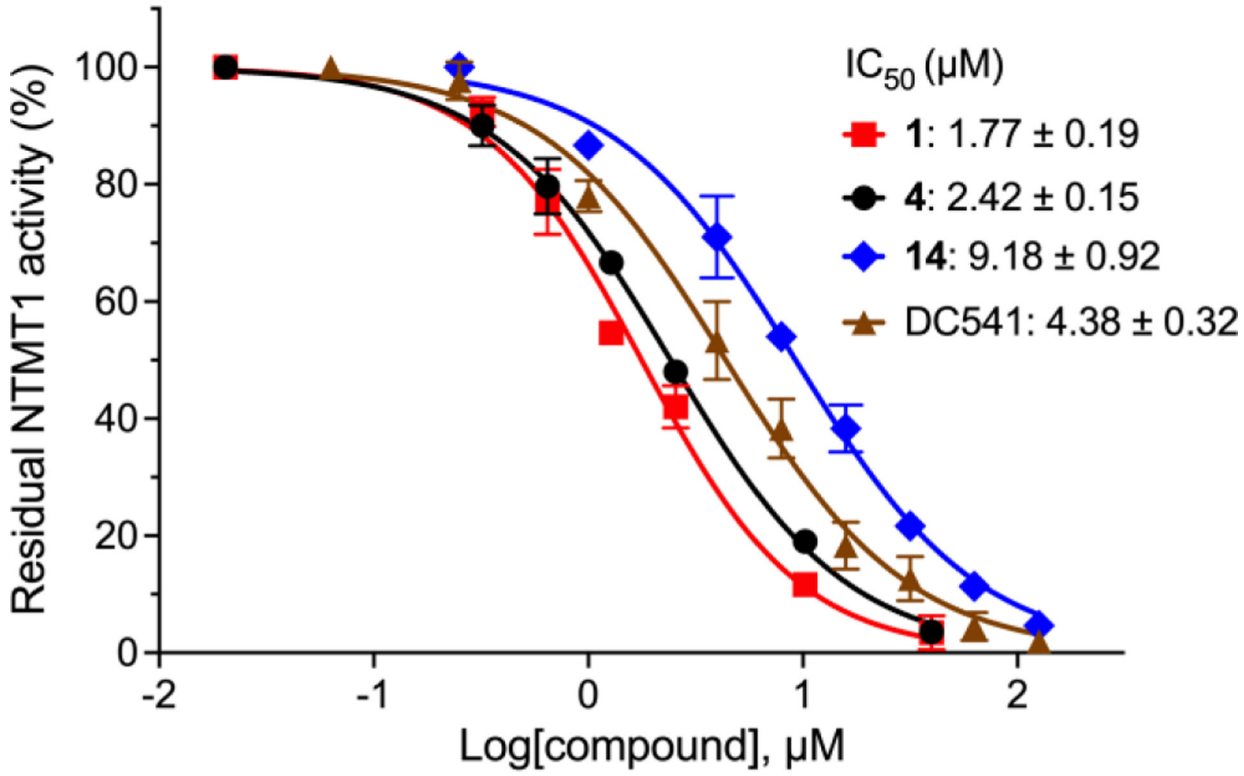

Figure 2.

Inhibition of NTMT1 *in vitro*. Experiments were performed in triplicate at 37 °C with NTMT1 (0.2 μM), RCC1 peptide (2 μM), SAM (6 μM), and various concentrations of degrader **1** (red), negative control **4** (black), DC541 (brown), and inhibitor **14** (blue). Values of IC_{50} are presented as mean ± standard deviation (SD).

Author Manuscript Author Manuscript Author Manuscript Author Manuscript

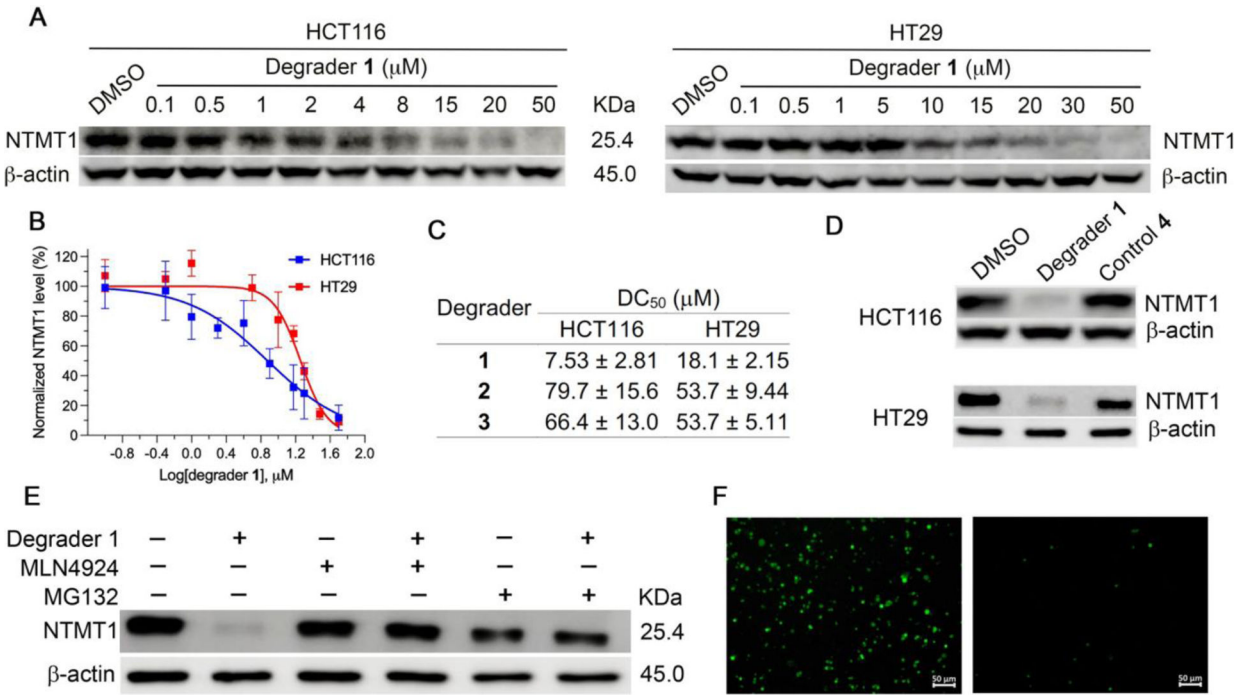

Figure 3.

Degradation of NTMT1 in colorectal carcinoma cell lines. (A) Western blots of dose-dependent degradation of NTMT1 in HCT116 (left) and HT29 (right) upon treating with degrader **1** for 24 h. (B) Quantification of NTMT1 levels relative to DMSO-treated controls in the presence of degrader **1** using ImageJ in HCT116 (blue line) and HT29 (red line). Each point represents three independent experiments. (C) Summary of DC_{50}. Values are presented as mean ± SD. (D) Western blots of NTMT1 in HCT116 (top) and HT29 (bottom) upon treating with 50 μM degrader **1** or negative control **4** for 24 h. (E) Western blots of NTMT1 in HCT116 treated with 1 μM MG132 or 1 μM MLN4924 for 2 h and then with 50 μM degrader **1** or DMSO for another 24 h. (F) Fluorescence microscopy of NTMT1-eGFP fusion protein overexpressed in HCT116. Cells were treated with the control DMSO (left) or 100 μM degrader **1** (right) for 24 h.

Author Manuscript Author Manuscript Author Manuscript Author Manuscript

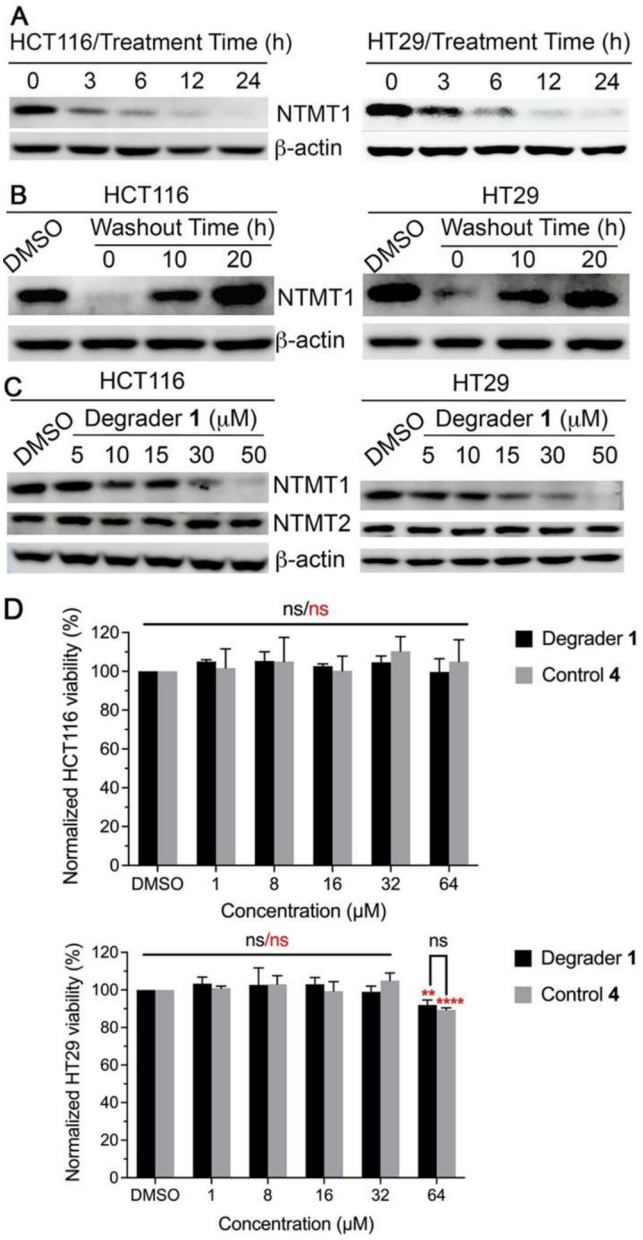

Figure 4.

Characterization of degrader **1** and negative control **4** in HCT116 and HT29 cells. All experiments were done in triplicates. (A) Western blots of time-dependent degradation of NTMT1 induced by degrader **1** at 50 μM. (B) Western blots of reversible NTMT1 degradation. Cells were treated with 50 μM degrader **1** for 24 h. Then the compound was washed out. NTMT1 recovery was monitored post the washout. (C) Selectivity of degrader **1**. Cells were treated with degrader **1** at various concentrations for 24 h and protein levels of NTMT1/2 were monitored by Western blots. (D) Cytotoxicity of degrader **1** and negative control **4** in HCT116 (top) and HT29 (bottom). Cells were treated with compounds at various concentrations for 24 h and their viability was assessed using a WST-8 assay. Statistical significance of comparisons was performed either between the degrader **1** and

Author Manuscript Author Manuscript Author Manuscript Author Manuscript

DMSO (labeled in red) or the degrader **1** and negative control **4** (labeled in black). Data are shown as mean ± SD ($p < 0.01$: **; $p < 0.0001$: ****; ns: not statistically significant).

Author Manuscript Author Manuscript Author Manuscript Author Manuscript

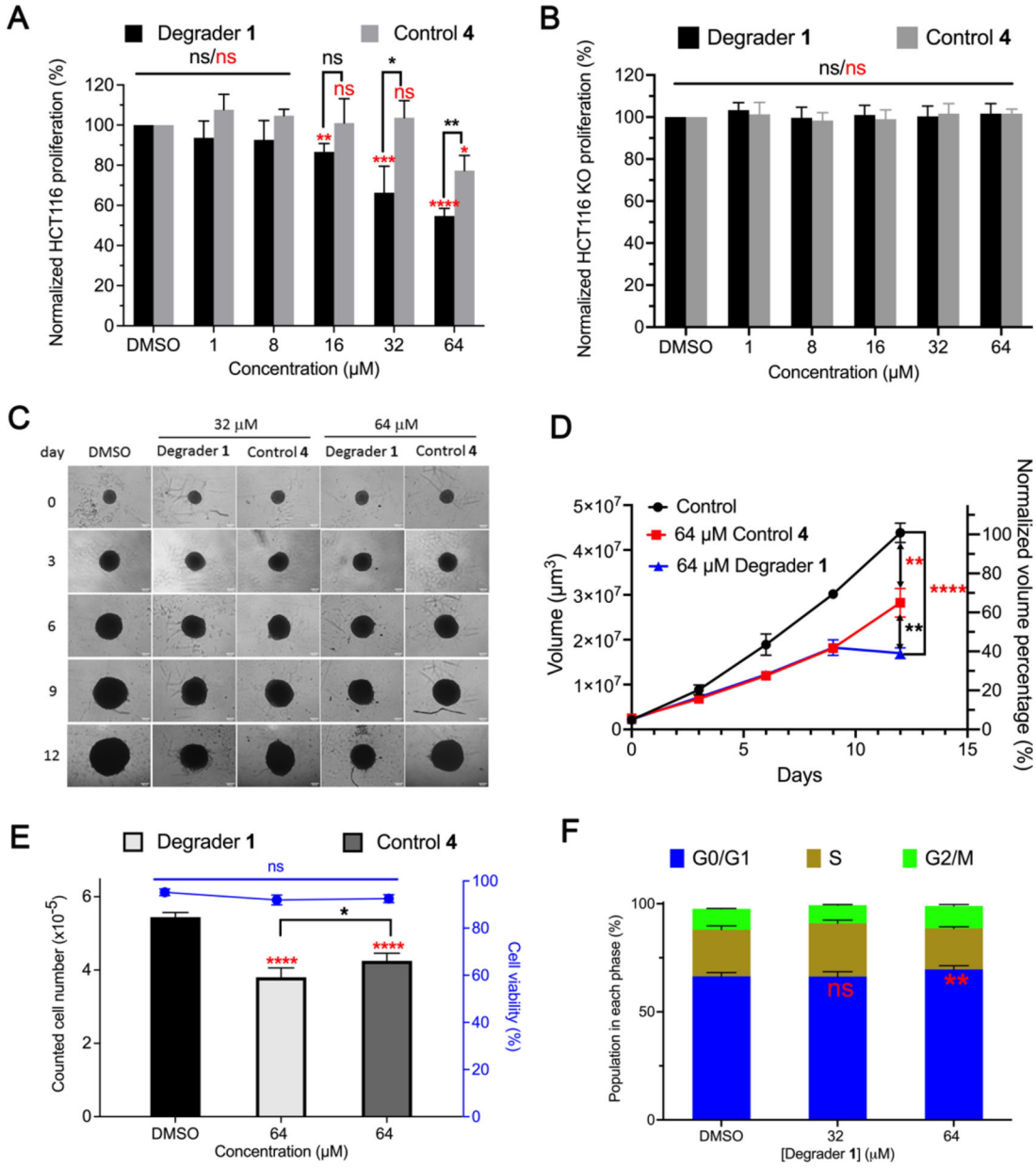

Figure 5.

Inhibition of HCT116 cell growth induced by degrader **1** and negative control **4**. All experiments were done in triplicates. Statistical significance of comparisons was performed either between degrader **1** and DMSO (labeled as red ns and *) or degrader **1** and negative control/inhibitor **4** (labeled as black ns and *). Data are shown as mean ± SD ($p < 0.05$: *; $p < 0.01$: **; $p < 0.001$: ***; $p < 0.0001$: ****; ns: not statistically significant) (**A**) Antiproliferative effects of degrader **1** (black) and control/inhibitor **4** (grey) at various concentrations after treating *wt* cells for 72 h. DNA was quantified by CyQUANT® assays (ThermoFisher). (**B**) Antiproliferative effects of degrader **1** (black) and control/inhibitor **4** (grey) at various concentrations after treating *ntmt1* KO cells for 72 h. (**C**) Representative images of cell spheroids treated with degrader **1** and negative control/inhibitor **4** at various

Author Manuscript Author Manuscript Author Manuscript Author Manuscript

concentrations or DMSO every three days. Cell culturing was performed in a 96-well plate with ultralow surface attachment. Scale bar: 100 μm. (**D**) Growth curves of cell spheroids shown in (**C**) at 64 μM. Spheroid volume was calculated according to the published protocol.[71] (**E**) Cell growth (bar column) in the presence of degrader **1** (light grey) and negative control/inhibitor **4** (dark grey) at various concentrations or DMSO for three days. Cell culturing was performed in peptide hydrogel PG-S (PepGel LLC). Cells were subject to AO/PI staining and then counted by automatic cell counting to determine the total numbers of live and dead cells. Cell viability was calculated as the percentages of live cells out of the total cells (blue curve). (**F**) Quantification of cells in each stage of the cell cycle by FlowJo. Cells were treated with degrader **1** for 72 h and then assessed for cell cycle distribution after PI staining.

Author Manuscript Author Manuscript Author Manuscript Author Manuscript

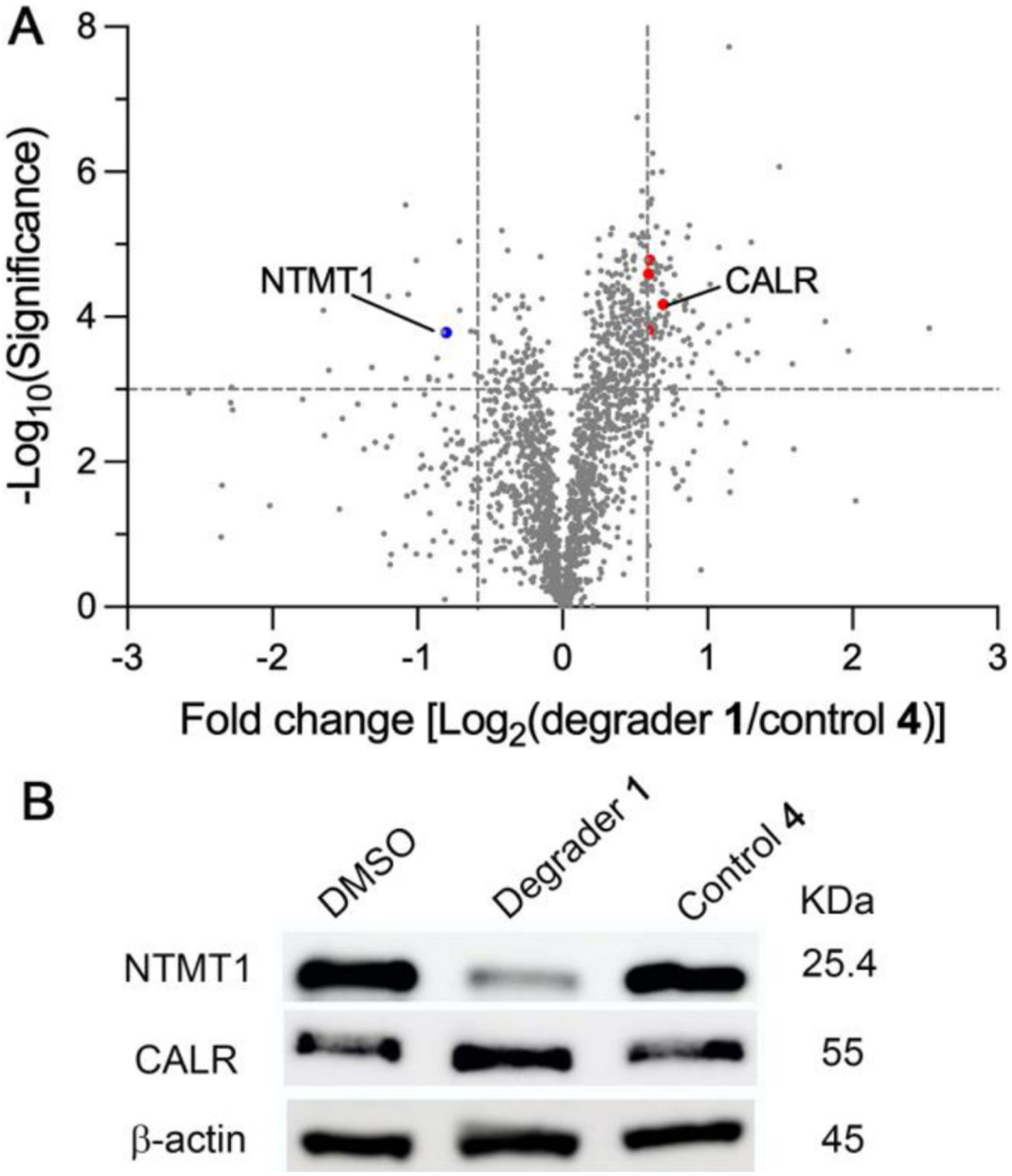

Figure 6.

Overexpression of CALR induced by degrader **1** in HCT116. Cells were treated with either degrader **1** or negative control/inhibitor **4** at 25 μM for 24 h. All experiments were done in triplicates. (A) Label-free quantitative global proteomic analysis and volcano plot of proteins undergoing expression level changes. Proteins with fold-change ≥ 1.5, significance ≤ 0.001, and number of unique peptides ≥ 4 are labeled as blue (downregulation) and red (upregulation) dots. MS data were analyzed using Progenesis QI for Proteomics (Waters). (B) Western blots of NTMT1 and CALR levels in cells treated with degrader **1** or control/inhibitor **4** at 25 μM for 24 h.

Author Manuscript Author Manuscript Author Manuscript Author Manuscript

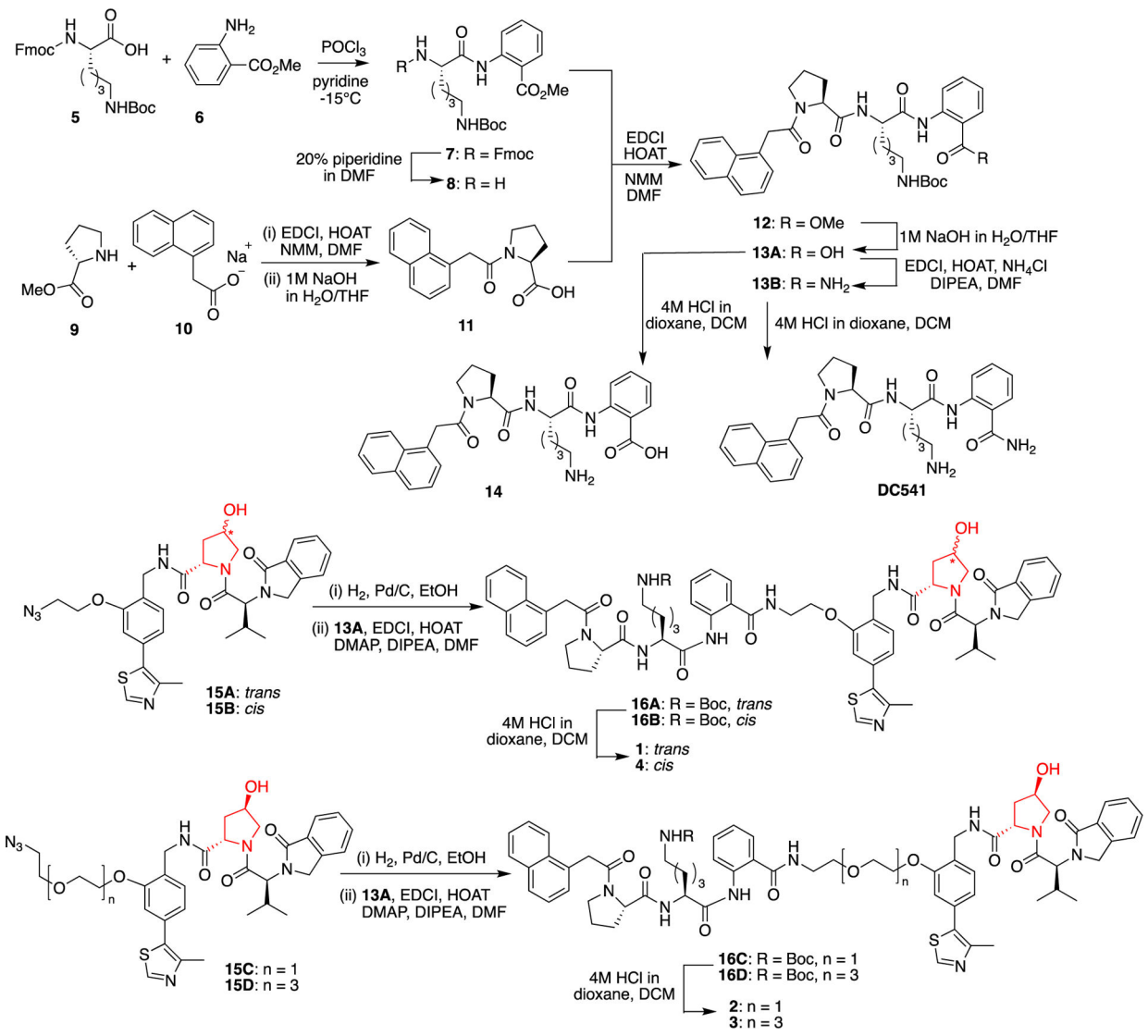

Scheme 1.

Synthetic route of NTMT1 PROTACs **1–3** and negative control/inhibitor **4**